2014

Freezing Curve Measurements For Hydrocarbon Mixtures

Derrick Amoabeng
North Carolina Agricultural and Technical State University

Freezing Curve Measurements for Hydrocarbon Mixtures

Derrick Amoabeng

North Carolina A&T State University

A thesis submitted to the graduate faculty

in partial fulfillment of the requirements for the degree of

MASTER OF SCIENCE

Department: Chemical, Biological and Bioengineering

Major: Chemical Engineering

Major Professor: Dr. Vinayak N. Kabadi

Greensboro, North Carolina

2014

The Graduate School
North Carolina Agricultural and Technical State University
This is to certify that the Master's Thesis of

Derrick Amoabeng

has met the thesis requirements of
North Carolina Agricultural and Technical State University

Greensboro, North Carolina
2014

Approved by:

Dr. Vinayak Kabadi Major Professor	Dr. Shamsuddin Ilias Committee Member
Dr. John P. Kizito Committee Member	Dr. Stephen Knisley Department Chairperson

Dr. Sanjiv Sarin
Dean, The Graduate School

Biographical Sketch

Derrick Amoabeng was born in Akim-Oda, Ghana on the 31st of May 1988. He received his Bachelor of Science degree in Chemical Engineering from Kwame Nkrumah University of Science and Technology – KNUST in Ghana in the year 2011. He is a candidate for the Master of Science degree in Chemical Engineering in North Carolina A&T State University, Greensboro, North Carolina.

Acknowledgements

I first of all want to thank the almighty God for how far He has brought me. He made all things possible. I would like to express my gratitude to my advisor, Dr. Vinayak Kabadi, for his continued support, encouragement, supervision and useful suggestion throughout this research work. His continued dedication to instilling discipline in me and his guidance enabled me to complete my work successfully. I am also thankful to my committee members, Dr. Vinayak N. Kabadi, Dr. John P. Kizito, Dr. Shamsuddin Ilias for being my committee members. I would also like to thank my colleagues, Mr. Emmanuel Ogbole and Mr. Thomas Anison for sharing research ideas and for their continued support, especially throughout the difficult times. Lastly, I would like to acknowledge NASA and Department of Chemical, Biological and Bio-engineering for providing financial support for this research.

Table of Contents

List of Figures

List of Tables

Abstract

Solid-liquid equilibrium measurements were carried out for a binary system of (decane + dodecane) at several different mole fractions under atmospheric pressure. The work involved the design of new experimental setup for the solid-liquid equilibrium data measurements. The newly designed setup was used to study the freezing curve and solid-liquid transition temperature for pure decane and dodecane as test runs. The main work was to investigate and confirm the binary mixtures which form solid solutions (solid state structure) or eutectic structures (each particular component forms crystals out of the solution separately), and further develop a binary solid-liquid phase diagram for decane and dodecane.

The experiment involved the use of an environmental chamber which housed a metal cell with the test liquid placed in it. Liquid samples were taken from the metal cell and analyzed in the Gas Chromatograph (GC) as the melting and freezing went on to determine their composition at various temperatures. The results from the experiment showed that the binary mixture forms a solid solution upon freezing. This was determined by withdrawing liquid samples from the metal cell and analyzing it in the GC as the liquid sample freezes. The liquid composition analyzed by the GC at every $2^{o}C$ temperature drop turned out to have the same composition as the initial composition placed in the metal cell. This shows that the binary mixture freezes together at a particular temperature. The temperature profiles of several mole fractions were determined and were used to develop the solid-liquid binary phase diagram for decane-dodecane mixture.

CHAPTER 1

Introduction

Solid-liquid equilibrium in alkane systems is a phenomenon of great interest in many industrial fields like the petroleum, pharmaceutical, and biotechnological industries among others. Efforts to model the solid-liquid equilibrium in these systems have been both empirical and with models with different degrees of success. The description of the solid phase non-ideality is the main obstacle in the modeling of the solid-liquid equilibrium of hydrocarbons. Broadhurst [1] has presented a detailed explanation of the solid state behavior of the entire n-paraffin series based on a comprehensive review of data available in the literature, and has identified four distinct crystal structures, of n-paraffin solids, these structures are hexagonal (rotator phase), monoclinic, triclinic and orthorhombic phases. Molecules of paraffin in hexagonal phase rotate about their long chain axes but those of monoclinic, triclinic and orthorhombic are greatly restricted.

The concept of local composition which is the core of local composition model was first reported by Wilson [2], who formulated the hypothesis according to which concentrations around two unlike central molecules would be different and dependent on the energies of interaction between the central and surrounding molecules. Wilson postulated that these local compositions would be related to the overall compositions through a Boltzman-type expression. The validity of the expression is not restricted to fluid phases but extends to all forms of condensed phases. Another local composition model called Chain Delta Lattice Parameter (CDLP) model was used by Milhet *et. al* [4] and Wilson equation to calculate the activity coefficient in the solid (rotator) phase for binary system. Both models lead to results in very

good agreement with experimental data for the rotator phases but the CDLP model was preferred because of its predictive characteristic.

Milhet *et. al* [4] stated that the orthorhombic solid phase is the most important crystalline structure present in alkane solid-liquid equilibrium or solid-solid equilibrium. The orthorhombic phase was assumed to be the main or only phase present in paraffinic deposit. Milhet *et. al* [4] assumed that the thermodynamic behavior of true hexagonal (rotator) phase is not substantially modified by the subsequent phase transitions and that the different phases can be considered identical. The local composition models provide good description of the orthorhombic phase. This made them use the Wilson equation for the description of the orthorhombic solid phase in alkanes and obtained good predictions for the solid-solid phase diagrams of systems of odd/odd, odd/even and even/even n-alkanes considering identical the multiple orthorhombic solid phases.

For mixed paraffin systems, which basically states that the solid solution of two alkanes is favored if the Gibbs free energy of the mixed crystal is lower than that of the crystals of the pure component; otherwise there is no mixing in the solid state and a eutectic is formed [5]. The conditions for solid solution formation also depend on molecular size and symmetry. That is, if the component alkanes are too different in length, then the mixture is fractionated into the separate pure crystals upon cooling from the melt. In the case of paraffins with nearly the same chain length, molecular and crystal symmetry are most important. Solid solutions are formed from multicomponent if the components are isomorphic and not of too different chain length so that no major lattice distortions are introduced when the components are mixed. In the case of n-paraffin this means that the symmetry of the total unit cell, including chain-end packing, in addition to the methylene subcell, is considered in an evaluation of miscibility.

Broadhurst [1] has prepared a table which contains the melting and transition temperature and also shows the phase transition structures for various n-paraffin as shown in the appendix A table A-1. In this work, the objectives are outlined as follows:

- To compile experimental data from literature of physical properties (saturation temperature, saturation pressure, specific heat capacity, and enthalpy of fusion) for pure and binary alkanes and cycloalkanes.
- To design and build an experimental apparatus for melting and freezing curve measurement.
- To measure solid-liquid transition temperature for pure decane and dodecane.
- To measure solid-liquid phase transition data for decane-dodecane binary system.
- To investigate and confirm if decane-dodecane system forms a solid solution.

This thesis has four additional chapters. Chapters 2 which is the literature review highlights on the various experimental data measured by researchers using various experimental setups. Also reviewed are activity coefficient models used to predict the non-ideality in solid and liquid multicomponent mixtures of paraffin. Chapter 3, which is the methodology describes in detailed the experimental setup used in the freezing curve measurement and gives the experimental procedure. Chapter 4 and chapter 5 which are the results and discussion respectively present the results from the experiments in the form of graphs. Analyses and discussion of experimental data are also presented.

CHAPTER 2

Literature Review

2.1 Solid-Liquid Equilibrium for Hydrocarbon Mixtures

The application of hydrostatic pressure is a factor that determines the freezing point temperatures and crystal formation of hydrocarbons and the complex mixtures. Increasing pressure results in high freezing temperatures for pure hydrocarbons, but it should be noted that an increase in pressure could cause a decrease in the freezing temperature if the hydrocarbon is a mixture rather than a pure component [6].

2.1.1 Literature Review on Experimental Methods and Data: Several studies have been done on the effect of pressure on the freezing temperature of pure, binary and multicomponent hydrocarbon mixtures. Various experiments have been carried out by researchers to report the solid-liquid equilibria (SLE) data on pure compounds, binary and multicomponent mixtures.

Various experimental setups were used by researchers to measure the solid-liquid equilibrium of hydrocarbon mixtures. We decided to design our own experimental setup to make use of the Tenney environmental chamber in the laboratory, which has a temperature range of -80^{o}C to 200^{o}C.

Our long term goal in this research is to study the freezing curves of aviation fuels, but to test our newly designed experimental setup, the solid-liquid equilibrium of binary system was first studied. There are several standard test methods for measuring the freezing point of aviation fuels. These test methods are ASTM D5972 [7], D7153 [8] and D2386 [9]. The ASTM D5972 is the standard test method for measuring the freezing point of aviation fuels using the automatic phase transition method. The ASTM D7153 is the standard test method for measuring the

freezing point of aviation fuels using automatic laser method. The ASTM D2386 is also a standard test method for measuring the freezing point of aviation fuels in a jacketed unsilvered vessel similar to a dewar flask.

Machado *et. al* [10] studied the thermal behavior upon heating for eicosane, tetracosane, triacontane and tetracontane between the pressures of (10 to 150) MPa. A transitiometer was used to measure the calorimetric signal, pressure and temperature at a very slow heating rate to guarantee thermal equilibrium. Among the above mentioned hydrocarbons, eicosane was the only one that did not present a solid-solid transition, the other compounds show a solid-solid transition a few Kelvin below the solid-liquid transition temperature.

Domańska and Morawski [11] determined the saturation temperature and pressure of [n-alkanes (tridecane, hexadecane, octadecane, eicosane) + cyclohexane] using a thermostated apparatus at very high pressure up to 1 GPa. It was observed that the freezing temperature of each mixture increases monotonously with increasing pressure. The eutectic point of the binary systems shifts to a higher temperature and to a higher n-alkane concentration with increasing pressure. Later that year, Morawski *et. al* [12] studied how to predict the SLE of the mixtures using only pure components data in a wide pressure range, far above the pressure range in which cubic equations of state are normally applied. The fluid phase was described by the corrected Soave-Redlich-Kwong (SRK)-Equation of State (EOS) using van der Waals one fluid mixing rules. The results of the predictions are compared with the experimental data

Wu *et. al* [6] studied the effect of pressure on the solidification of several saturated cyclic hydrocarbons and three xylene isomers. A variable-volume view cell at pressures to 300MPa and temperatures starting at 293.15 K was used for the experiment. Solid–liquid transitions were observed for cyclooctane, cis-1,2-dimethylcyclohexane, trans-1,4-dimethylcyclohexane, p-

xylene, o-xylene, and 2-methylnaphthalene. However, methylcyclohexane, ethylcyclohexane, cis-1,4-dimethylcyclohexane, and m-xylene remained liquid over the same operating pressure and temperature ranges. The variable volume view cell is used in the measurement of solid-liquid phase transitions under high pressure. The internal volume of the cell is adjusted with a pressure generator that injects water behind the o-ring-sealed piston. The cell is loaded with the hydrocarbon of interest and the gas volume in the cell is eliminated by moving the piston forward until liquid hydrocarbon is ejected from the top port of the cell. The cell contents are viewed on a TV monitor using a camera connected to a borescope placed against a sapphire window secured at one end of the cell. This apparatus allows for visual determination of any water leakage around the piston o-ring since water has a very small solubility in the hydrocarbons considered in this study. If water is detected, the apparatus is disassembled, cleaned, and reloaded A typical schematic diagram of a variable volume view cell is shown in Figure 2-1.

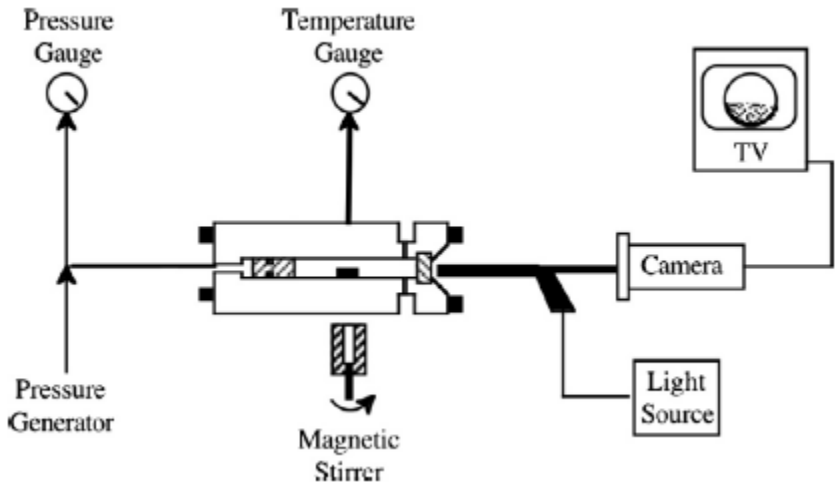

Figure 2-1, Schematic diagram of high pressure view cell system

The solid-liquid phase behavior for benzene and n-alkanes in binary systems (C_6H_6 + n-$C_{14}H_{30}$), (C_6H_6 + n-$C_{16}H_{34}$), (C_6H_{12} + n-$C_{14}H_{30}$) and (C_6H_{12} + n-$C_{16}H_{34}$) at temperatures from

230 to 323K and pressures up to 120MPa was studied by Tanaka and Kawakami [13]. The experiment was done by visual observation of the phase transition using high pressure optical vessel with the aid of a video microscope.

A general review was done by Dirand *et. al* [14] for temperatures and enthalpies of (solid+solid) and (solid+liquid) transitions of pure normal alkanes are presented. Mean values are determined from literature data on pure normal alkanes for methane up to the alkane of carbon atom number *n* equal to 390.

Machado and de Loos [15] also presented experimental work of vapor-liquid and solid-fluid equilibrium data for 13 different compositions of the system methane + triacontane. The data presented covered the temperature range from 315 to 450 K and pressures up to 200MPa with almost pure compositions of methane to pure triacontane. Milhet *et. al* [4] studied the crystallization temperatures of two binary systems – (tetradecane + hexadecane and tetradecane + pentadecane) under high pressure up to 100MPa using a polar microscopy device. The slopes of the melting curves in the (T, P) diagram show a dependence on the nature of the different solid phases that can appear. Flöter *et. al* [16] also presented experimental vapour-liquid, solid-fluid, and solid-liquid-vapor equilibrium data of the binary system (methane + tetracosane) in the temperature range 315 – 415K and for pressure up to 200MPa. The experiments were done for various mixtures with compositions ranging from almost pure methane to pure tetracosane. It was found that the (solid α- solid β) transition of pure tetracosane had hardly any influence on the shape of the (solid + fluid/fluid) boundary curves and three phase equilibrium curve (solid tetracosane + liquid + vapor) of the binary system.

Domanska and Morawski [17] measured solid-liquid equilibria at temperature greater than 280 K for several n-alkanes and the experimental results were compared with values

calculated by means of the Wilson, UNIQUAC and NRTL equations utilizing parameters derived from the experimental solid-liquid equilibria. Khimeche *et. al* [18] reported binary solid–liquid equilibria for [naphthalene + (eicosane, pentacosane, hexatriacontane)] mixtures by differential scanning calorimetry. The results were compared with those from modified UNIFAC (Larsen and Gmehling versions) and ideal predictions.

Yang *et. al* [19] investigated the solid-liquid equilibria of (1-octanol + n-alkane) systems at temperatures from 268 to 333K and pressures up to 220MPa by the visual observation with a high-pressure optical vessel. The solid-liquid coexistence curve and the eutectic points were found to increase to higher temperatures monotonically with increasing pressure in these systems.

Gregorowicz [20] analyzed the criteria for the existence of the retrograde melting temperature phenomena in terms of volumetric and enthalpic properties of the coexisting phases. The analysis was bases on Gibbs-Konovalow equations and was supported by new experimental results for the system propane + tetrecontane and literature data.

Experimental data on solid-liquid equilibria for pure hydrocarbon (n-alkanes) compounds and binary systems is shown in Appendix A. Table A-1 shows melting and transition temperatures for n-paraffins. It shows the different types of solid structures formed by the various numbers of carbons in chains. Experimental data of physical properties (saturation temperature, saturation pressure and enthalpy of fusion) for pure hydrocarbons are tabulated in Table A-2. Specific heat capacity data for solids and liquids of pure hydrocarbons are shown in Table A-5, A-6 and A-7. Table A-3 shows experimental data of solid-liquid equilibrium for binary hydrocarbon mixtures and Table A-8 shows extracted solid-liquid equilibrium data for pure hydrocarbons.

2.1.2 Thermodynamic Modeling of Solid-Liquid Equilibrium: The modeling of crystal formation in hydrocarbon fluids is based on the thermodynamic description of the equilibrium between the solid and liquid phases. The thermodynamic equilibrium relates to the solid and liquid fugacity. Based on the solid solution approach, the following equation is satisfied at the equilibrium

$$f_i^S\left(P,T,x_i^S\right)= f_i^L\left(P,T,x_i^L\right) \tag{1}$$

In equation (1), $f_i^S\left(P,T,x_i^S\right)$ and $f_i^L\left(P,T,x_i^L\right)$ are the fugacity of component in the solid and liquid phases in pressure P, temperature T and mole fraction x_i^S and x_i^L respectively. The fugacity in the liquid and solid phases is calculated by the following equations;

$$f_i^L\left(P,T,x_i^L\right)= x_i^L\, f_{purei}^L \gamma_i^L \tag{2}$$

$$f_i^S\left(P,T,x_i^S\right)= x_i^S\, f_{purei}^S \gamma_i^S \tag{3}$$

The f_{purei} and γ_i are the fugacity of pure component i and its activity coefficient in the mixture while superscripts of l and s are related to the liquid and solid phases, respectively. The solid and liquid equilibrium ratio for component i is defined as follows;

$$K_i^{SL} = \frac{x_i^S}{x_i^L} = \frac{f_{purei}^{\mathrm{L}}(P,T)\gamma_i^L\left(P,T,x^L\right)}{f_{purei}^{\mathrm{S}}(P,T)\gamma_i^S\left(P,T,x^S\right)} \tag{4}$$

The relation between pure solid and liquid component fugacity can be obtained using equation (5) [21]:

$$\left(\frac{f_{purei}^L(P,T)}{f_{purei}^S(P,T)}\right) = \exp\left(\frac{\Delta H_i^f}{RT}\left(1-\frac{T}{T_i^f}\right)+\frac{\Delta H_i^{OD}}{RT}\left(1-\frac{T}{T_i^{OD}}\right)-\frac{1}{R}\int_T^{T_i^f}\frac{\Delta Cp_i^{SL}}{T}dT+\frac{1}{RT}\int_T^{T_i^f}\Delta Cp_i^{SL}dT\right) \tag{5}$$

Several researchers introduced modification to the fugacity ratio equation in equation (5) to simplify it. Won [22] model introduced simplifications in equation (5). The variation of heat

capacity was neglected as it provides only a slight contribution in the exponential function and the melting temperatures and solid–solid transition temperatures are considered as equal since they are generally very close [23]. Schou Pedersen *et. al* [24] improved Won [22] model by taking into account the heat capacity difference between hydrocarbons in the liquid and solid states. With this modification reasonable results were obtained. Ungerer *et. al* [25] proposed the heavy components of a hydrocarbon mixture crystallizes pure with several solid phases. Therefore, the fugacity of the pure component i in the solid state is determined from the fugacity of the same substance in the sub-cooled liquid state. Ghanaei *et. al* [26] also neglected the heat capacity terms and substituted the Clapeyron's equation into the change in molar volume term of component i in the liquid and other solid phases in the fugacity ratio equation. Experimental values of pressure-temperature (P-T) saturation slope in the solid-liquid and solid regions were used in the Clapeyron's equation.

The solid-liquid transition curve can be predicted by using reliable thermodynamic models. In hydrocarbon mixtures, the non-idealities arise from both entropic effects such as size difference and free volume effects and energetic interactions between unlike molecules as aromatics and aliphatics [27]. There are several thermodynamic models that can be used to predict the activity coefficients of each component in the liquid and solid phases.

Won [22] used regular solution theory to describe the non-idealities in the oil (liquid) and wax (solid) phases. Won [28] used a combination of regular solution theory and Flory-huggins models for the description of non-ideality liquid phase behavior. Hansen et al applied polymer solution theory of Flory for the oil phase while the liquid phase was assumed to be an ideal mixture. Schou Pedersen *et. al* [24] also proposed a regular solution theory with a little modification on the fugacity ratio equation. Esmaeilzadeh *et. al* [21] stated that recent studies

have shown that a normal paraffin mixture with a consecutive carbon number distribution forms a single orthorhombic solid solution. Coutinho *et. al* [29], [30] evaluated several approaches for calculating activity coefficients including UNIFAC, Flory-Huggins, Flory free-volume and entropic free volume. Coutinho and Ruffier-Méray [31] presented a model based on the Flory-free-volume model for the liquid phase and on the predictive local composition model, a predictive form of the Wilson equation for the non-ideality of the solid solution.

The following year, Coutinho [27] published another thermodynamic model in which the UNIQUAC model and a combination of UNIFAC and the Flory free-volume approach were used for the calculation of activity coefficients in solid and liquid phases, respectively. Pauly *et. al* [32] described the fluid phase behavior by using a modified LCVM, an equation of state–G^E model and the solid phase non-ideality is represented by the Wilson equation using the predictive local composition concept. Esmaeilzadeh *et. al* [21] investigated the performance of several activity coefficient models and found appropriate set of activity coefficient models for the description of solid and liquid phases in wax formation phenomena in alkane mixtures. Their results proved that the predictive Wilson, together with one of the models, regular solution, UNIFAC, predictive UNIQUAC was more appropriate for the description of the no-ideality solid and liquid phase behavior.

2.1.3 Activity Coefficient Models: Some the original activity coefficient models have been modified by researches since they were developed to improve its performance against experimental data. The activity coefficient models are Regular Solution Theory, UNIQUAC, UNIFAC, NRTL and Wilson's equation.

2.1.4 Non-Random Two Liquid-NRTL: The NRTL model which is an example of a local composition model is defined as follows [33]

$$\frac{g^E}{RT} = \sum_{i=1}^{n} x_i \sum_{k=1}^{n} \frac{x_j \exp\left(-\alpha \frac{\lambda_{ij} - \lambda_{ii}}{RT}\right)}{\sum_{k=1}^{n} x_k \exp\left(-\alpha \frac{\lambda_{ki} - \lambda_{ii}}{RT}\right)} \frac{\left(\lambda_{ij} - \lambda_{ii}\right)}{RT} \tag{6}$$

The parameter α is a measure of the non-randomness of the mixture. $\alpha = 2/z$, z being the co-ordination number

2.1.5 UNIQUAC: The UNIQUAC model was originally developed by Abrams and Prausnitz as a generalization of Guggenheim's quasi-chemical theory through the introduction of local area fractions as the primary concentration variable, and the use of Staverman's combinatorial entropy as boundary condition for athermal mixtures. It can be written as [33]

$$\frac{g^E}{RT} = \sum_{i=1}^{n} x_i \ln\left(\frac{\Phi_i}{x_i}\right) + \frac{Z}{2} \sum_{i=1}^{n} q_i x_i \ln \frac{\theta_i}{\Phi_i} - \sum_{i=1}^{n} x_i q_i \ln\left[\sum_{j=1}^{n} \theta_j \exp\left(-\frac{Z}{2} \frac{\lambda_{ij} - \lambda_{ii}}{q_i RT}\right)\right] \tag{7}$$

with

$$\theta_i = \frac{x_i r_i}{\sum_j x_j r_j} \text{ and } \theta_i = \frac{x_i q_i}{\sum_j x_j q_j} \tag{8}$$

Another important issue to be addressed in applying the UNIQUAC model to the solid phase is the evaluation of the structural parameters *r* and *q*. They were originally defined in such a way as to be proportional to the van der Waals volume and area of a methylene group. This is correct for a fluid phase where the unit of interaction of two molecules can easily be assumed to be the methylene group. It should not be the case, however, for a chain molecule in a crystal lattice where the interaction takes place as a whole along the contact area between two molecules. The *r* and *q* parameters should then be redefined to incorporate the actual contact unit for the solid phase. Coutinho [33] reported two ways of calculating the r and q values. For the first case, an approach was used to estimate the volume and area of a cylinder of 25 methylene units considered to be a representative interaction unit for alkanes. It yielded a standard segment

volume of 58.39cm^3/mol and a standard segment area of 11.56×10^9 cm^2/mol that provides the new values for r and q:

$$r_i = \frac{V_{wi}}{58.39} \text{ and } q_i = \frac{A_{wi}}{11.56\times10^9} \tag{9}$$

Another simpler, but more empirical approach was used by defining the new interaction units as having 10 of the original methylene units and thus the new r and q values are obtained by dividing the original r and q values by the respective values for 10 methylene units:

$$r_i = \frac{r_{iorg}}{6.744} \text{ and } q_i = \frac{q_{iorg}}{5.40} \tag{10}$$

Another empirical equation was reported by Esmaeilzadeh *et. al* [21] which is a correlation of r and q values with the n-alkane chain length.

$$r_i = 0.01148\,C_{ni} + 0.00996 \tag{11}$$

$$q_i = 0.0185\,C_{ni} + 0.0211 \tag{12}$$

The interaction energy, λ_{ii} is estimated from the heat of sublimation of pure orthorhombic crystal:

$$\lambda_{ii} = -\frac{2}{Z}\left(\Delta H_{sub\,i} - RT\right) \tag{13}$$

For orthorhombic crystal, the value of Z is considered as 6 [21]. The interaction energy between two non-identical molecules is given by

$$\lambda_{ij} = \lambda_{ji} = \lambda_{jj} \tag{14}$$

The j is the n-alkane with the shorter chain of the pair ij and $\Delta H_{sub\,i}$ is the heat of sublimation.

2.1.6 Regular Solution Theory: In regular solution theory, the activity coefficient is calculated from the equations below [21]:

$$\ln \gamma_i = \frac{V_i\left(\bar{\delta} - \delta_i\right)^2}{RT} \tag{15}$$

Where V, δ and $\bar{\delta}$ are the molar volume, solubility parameter and average solubility parameter respectively. The values of $\bar{\delta}$, φ_i^L and φ_i^S can be obtained from the following relations:

$$\bar{\delta} = \sum_i \varphi_i \delta_i \tag{16}$$

$$\varphi_i^L = \frac{x_i^L V_i^L}{\sum_i x_i^L V_i^L} \qquad \varphi_i^S = \frac{x_i^S V_i^S}{\sum_i x_i^S V_i^S} \tag{17}$$

As φ_i^L and φ_i^S are the volume fraction of liquid and solid phases, respectively. In this approach, the liquid and solid molar volumes are assumed to be equal. Therefore

$$V_i^L = V_i^S = V_i = \frac{MW_i}{d_{i,25}^L} \tag{18}$$

For estimation of the liquid density of each component at 25°C $\left(d_{i,25}^{\mathrm{L}}\right)$, the following correlation depending on the molecular weight was proposed by Schou Pedersen *et. al* [24].

Solubility parameters in the liquid and solid phases $\left(\delta_i^L \text{ and } \delta_{\mathrm{i}}^{\mathrm{S}}\right)$ related to carbon number $\left(C_{ni}\right)$ are calculated by the immediate equations suggested by Schou Pedersen *et. al* [24].

$$\delta_i^L = 7.41 + 0.5194\left(\ln C_{ni} - \ln 7\right) \tag{19}$$

$$\delta_i^S = 8.5 + 5.763\left(\ln C_{ni} - \ln 7\right) \tag{20}$$

2.1.7 Wilson's Equation: In Wilson equation which is a local composition model equation, the activity coefficient can be calculated as shown below [34]:

$$\frac{g^E}{RT} = -\sum_{i=1}^{m} x_i \ln\left(\sum_{j=1}^{m} x_j \Lambda_{ij}\right) \tag{21}$$

$$\Lambda_{ij} = \frac{v_j}{v_i}\exp\left(-\frac{\lambda_{ij}-\lambda_{ii}}{RT}\right) \quad \Lambda_{ji} = \frac{v_i}{v_j}\exp\left(\frac{\lambda_{ji}-\lambda_{jj}}{RT}\right) \tag{22}$$

The activity coefficient for any component k is given by

$$\ln\gamma_k = 1 - \ln\left(\sum_{j=1}^{m} x_j \Lambda_{kj}\right) - \sum_{i=1}^{m} \frac{x_i \Lambda_{ik}}{\sum_{j=1}^{m} x_i \Lambda_{ij}} \tag{23}$$

The predictive version of Wilson's equation has been developed by Coutinho and Stenby [30]. The model is basically a version of the Wilson's equation where local mole fractions are employed as shown in the equation below:

$$\frac{g^E}{RT} = -\sum_{i=1}^{m} x_i \ln\left(\sum_{j=1}^{m} x_j \Lambda_{ij}\right) \tag{24}$$

$$\Lambda_{ij} = \frac{x_j}{x_i}\exp\left(-\frac{\lambda_{ij}-\lambda_{ii}}{RT}\right) \tag{25}$$

2.1.8 UNIFAC: A group-contribution method, called UNIFAC has been developed for estimating activity coefficients in nonelectrolyte liquid mixtures. The activity coefficient consists of two parts: the combinatorial contribution, due mostly to differences in molecular size and shape, and the residual contribution, arising mostly from differences in the intermolecular forces of attraction. For a component i in a multicomponent solution [35].

$$\ln\gamma_i = \ln\gamma_i^C + \ln\gamma_i^R \tag{26}$$

$$\ln \gamma_i^C = \ln \frac{\phi_i}{x_i} + \frac{z}{2} q_i \ln \frac{\theta_i}{\phi_i} + l_i - \frac{\phi_i}{x_i} \sum_j x_j l_j \tag{27}$$

Where

$$l_i = \frac{z}{2}(r_i - q_i) - (r_i - 1) \tag{28}$$

The coordination number z is taken to be 10. The area fraction θ and the segment fraction ϕ are related to the mole fraction x through

$$\theta_i = \frac{q_i x_i}{\sum_j q_j x_j} \qquad \phi_i = \frac{r_i x_i}{\sum_j r_j x_j} \tag{29}$$

Where pure-component parameters r_i and q_i are, respectively, measures of molecular (van der Waals) volumes and molecular surfaces areas. These, in turn, are given by group contributions R_k and Q_k according to

$$r_i = \sum_k \nu_k^{(i)} R_k \qquad q_i = \sum_k \nu_k^{(i)} Q_k \tag{30}$$

Where $\nu_k^{(i)}$, always an integer, is the number of groups of type of k in molecule i. The residual contribution to activity coefficient γ_i is given by

$$\ln \gamma_i^R = \sum_{\substack{k \\ all\ groups\ in \\ the\ solution}} \nu_k^{(i)} \left[\ln \Gamma_k - \ln \Gamma_k^{(i)} \right] \tag{31}$$

Where Γ_k is the group residual activity coefficient of group and $\Gamma_k^{(i)}$ is the residual activity coeffiecient of group k in a reference solution containing only molecules of type i. The group residual activity coefficient is related to the composition and temperature through

$$\ln \Gamma_k = Q_k \left[1 - \ln \sum_m \theta_m \psi_{mk} - \sum_m \left(\theta_m \psi_{km} \Big/ \sum_n \theta_n \psi_{nm} \right) \right] \tag{32}$$

In the above equation, θ_m is the area fraction of group m and the sums are over all groups.

$$\theta_m = \frac{Q_m X_m}{\sum_n Q_n X_n} \tag{33}$$

$$\psi_{mn} = \exp - \left[\frac{U_{mn} - U_{nn}}{RT} \right] = \exp - \left(\frac{a_{mn}}{T} \right) \tag{34}$$

Where X_m is a measure of the energy of interaction between groups m and n. The group interaction parameters a_{mn} and a_{nm} $\left(a_{mn} \neq a_{nm}\right)$ have been systematically evaluated from a large body of vapor-liquid and liquid-liquid equilibrium data.

Esmaeilzadeh *et. al* [21] stated that, for mixtures containing alkanes only, the residual term of UNIFAC is assumed to be zero. Therefore, the activity coefficient equation of UNIFAC for a mixture that contains different alkanes is represented by only the combinatorial term. Thus:

$$\ln \gamma_i = \ln\left(\frac{\Phi_i}{x_i} \right) + 1 - \frac{\Phi_i}{x_i} - \frac{Z}{2} q_i \left(\ln\left(\frac{\Phi_i}{\theta} \right) + 1 - \frac{\Phi_i}{\theta_i} \right) \tag{35}$$

The r and q values were also presented in an empirical form from data fitting from experimental values.

$$r_i = 0.6744\, C_{ni} + 0.4534 \tag{36}$$

$$q_i = 0.54 C_{ni} + 0.616 \tag{37}$$

Coutinho *et. al* [36] developed another model called the Chain Delta Lattice Parameter model (CDLP). This model was developed for the description of solid-liquid equilibrium of n-alkanes ranging from n-C_{20} to n-C_{40}. It was proven that, when the CDLP model is applied to systems with a symmetric behavior, it yields a correct description of both the enthalpic and entropic parts of the excess Gibbs free energy. The CDLP model can be expressed as follows [3]:

$$g^E = 2317 \frac{(l_l - l_s)^3}{l_s^3} x_1 x_s \text{ kJ/mol} \quad (38)$$

where l_l and l_s are the length of the long and short alkane molecules in the rotator phase respectively calculated using the following correlation:

$$l_i = 1.270 Cn_i + 1.98 \quad (39)$$

CHAPTER 3

Methodology

3.1 Experimental Setup

The experimental set-up has been designed in such a way that there is an environmental chamber which serves as a refrigeration unit for freezing and melting the sample. The environmental chamber houses the test cell which contains the hydrocarbon mixture. The test cell has an overhead stirrer and a thermocouple inserted in it. The metal cell is connected to a metering valve with 1/16 inch stainless steel tubing. The 1/16 inch stainless steel tubing from the metering valve is inserted into a bottle through a cork. The bottle is connected to a vacuum pump with a pipe to create vacuum of in the bottle. This then forces the liquid to move from the metal cell into the bottle. During the experiment, liquid samples are withdrawn at desired time interval from the test cell through a 1/8 inch Swagelok T-shaped fitting. The withdrawn liquid sample is diluted and injected into the 8610C Gas Chromatograph which is used to determine the composition of the hydrocarbon mixture in the test cell that is yet to crystallize as the temperature decreases. The drawing for the experimental setup is shown in Figure 3-1 below.

3.1.1 Chemical and Materials: The pure compounds (decane, dodecane and hexadecane) used in this work were purchased from Sigma Aldrich, with purities better than 99wt% and were used without further purification. The fittings, unions, Nupro filter and metering valve used in this experiment were supplied by Swagelok. The reducing ferrules and other fittings were also supplied by Valco Instruments Company Incorporated. The metal test cell was manufactured by Mechanical Specialty Company. All these materials were made of stainless steel.

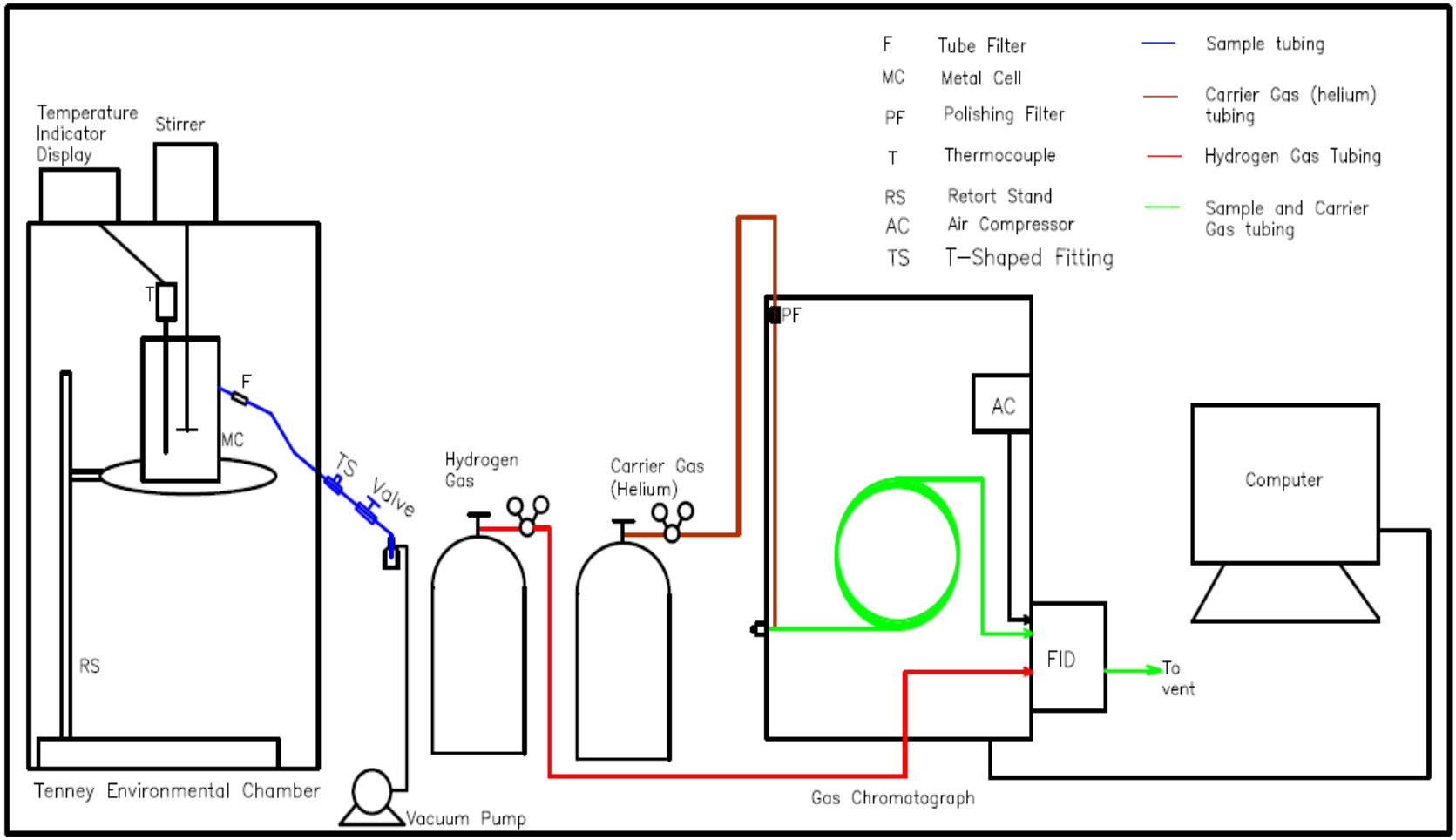

Figure 3-1, The Experimental Setup

3.2 Description of Gas Chromatograph and Environmental Chamber:

An SRI 8610C gas chromatograph equipped with a Flame Ionization Detector was used in this experiment. Certain parameters must be set for proper operation of the GC unit. These parameters included verifying the flow of carrier gas (helium gas), setting the ratio of air to hydrogen flow to the required ratio and setting the temperature of the column and detector. Other parameters could be set from the accompanying peak-simple software which included temperature ramping profiles, setting individual component details and peak detection sensitivity (area reject). The GC was modified with an injection port with 26 gauge needle size with a packed column installed in the oven. The oven is then connected to an FID.

The SRI online document for Flame Ionization Detector describes it as a detector that responds to any molecule with a carbon-hydrogen bond, but its response is either poor or nonexistent to compounds such as H_2S, CCl_4, or NH_3. Since the FID is mass sensitive, not concentration sensitive, changes in carrier gas flow rate have little effect on the detector response. It is preferred for general hydrocarbon analysis, with a detection range from 0.1ppm to almost 100%. The FID's response is stable from day to day, and is not susceptible to contamination from dirty samples or column bleed. It is generally robust and easy to operate, but because it uses a hydrogen diffusion flame to ionize compounds for analysis, it destroys the sample in the process.

The FID features a unique ceramic igniter which can run hot continuously. This ignitor is positioned perpendicular to the stainless steel detector jet and does not penetrate the flame. Opposite this flame is the collector electrode. This positively charged metal tube serves as a collector for the ions released as each sample component elutes from the column and is pyrolyzed in the flame; it doubles as a vent for the FID exhaust gas. The FID is equipped with an

electrometer amplifier which has high, high (filtered), and medium gain settings. The hydrogen and air gas flows are controlled using electronic pressure controllers, which are user adjustable via the GC's front panel. A thermostatted aluminum heater block maintains a stable detector temperature which is user adjustable up to 375^{o}C.

In the FID, the carrier gas effluent from the GC column is mixed with hydrogen, and then routed through a stainless steel jet. The hydrogen mix supports a diffusion flame at the jet's tip which ionizes the analyte molecules. Positive and negative ions are produced as each sample component is eluted into the flame. A collector electrode attracts the negative ions to the electrometer amplifier, producing an analog signal for the data system input. An electrostatic field is generated by the difference in potential between the positively charged collector electrode and the grounded FID jet. Because of the electrostatic field, the negative ions have to flow in the direction of the collector electrode.

The Tenney environmental chamber is used as the refrigeration unit in this experiment. It can be operated from a front panel with the temperature range of -80^{o}C to 200^{o}C.

3.2.1 Gas Chromatography Method: The first step in setting up the GC for a typical run is to verify the presence of carrier gas (helium) flow through the column. The helium and hydrogen gas cylinder regulators are set to 40psi to allow enough flow of gas to the GC. The GC has only one detector which is an FID. The Ultra high purity helium gas flow was then set at 7psi from the front panel of the GC, with that of Ultra-pure hydrogen gas set at 24psi. Additionally, the internal air compressor's flow rate was set to 5psi. From the above pressure values, a volumetric flow rate of 250ml//min and 25ml/min was set for the air and hydrogen respectively to produce a flame in the FID when the FID igniter switch is flipped up. The volumetric ratio of air to hydrogen in the flame port zone must be approximately 10:1. A characteristic pop that

resonate from the flame port indicates that the combustion has occurred. The condensation of water vapor on a wrench signifies that the FID is in operation and can be used to detect samples injected into the FID.

A temperature ramping program was employed for the column and the temperature profile was set via the peak simple software under edit channel 1 for temperature control dialog box. The parameters for each major section of the GC are shown below:

Column Temperature Ramping:

- Initial Temperature: 35^{o}C
- Ramp rate: 10^{o}C/min
- Final Temperature: 300^{o}C
- Hold: 300^{o}C for 5mins
- Column Type: Packed Column (Sim-Dist 2887)
- Carrier gas flow rate: 35ml/min

FID Detector Settings

- Detector Temperature: 150^{o}C
- Gain Setting: High
- Hydrogen flow rate: 25ml/min
- Air flow rate: 250ml/min

Table 3-1, Component Window:

Peak ID	Name	Retention Window	
		Start (min)	End (min)
1	Decane (C_{10})	2.65	4.47
2	Dodecane (C_{12})	5.75	7.55
3	Hexadecane (C_{16})	11.00	13.15

3.2.2 Calibration of Gas Chromatograph (GC) – Flame Ionization Detector (FID): GC-FID is calibrated using a standard solution prepared with decane, dodecane, hexadecane and hexane. Hexane is used as the solvent, decane, dodecane and hexadecane as solutes. A 1000ppm standard solution which contains the three solutes is prepared with hexane as the solvent.

To prepare a 1000ppm solution; 10µl of the individual solutes are injected into a 10ml of hexane with a syringe into a 20ml vial. The solution is gently shaken to form a homogenous mixture and kept in a refrigerator for about 2 to 3 hours. The solution is gently shaken again and left undisturbed in the refrigerator for 20mins to allow the component molecules to mix properly. The 1000ppm solution is injected with 1.0µl syringe into the GC with 0.5µl and 1.0µl injected three times each to calculate the average calibration constant (Area/Mole) for each solute

The calibration constant is used as a reference for calculating the mole fractions of hydrocarbons in an unknown mixture but have the peak area of the individual solutes. The calibration constant for each solute is also calculated relative to that of decane. The table below shows calibration constant (Area/Moles) for each amount of solution injected with the Area/Mole ratio relative to that of decane (calibration constant ratio). The peaks area of an unknown solute composition is also expressed in area ratio relative to that of decane. The individual area ratios are divided by their corresponding calibration constant ratio to get the mole fraction relative decane.

The Figure 3-2 is gas chromatogram run for 1.0µl manually injected for the standard solution prepared for calibration.

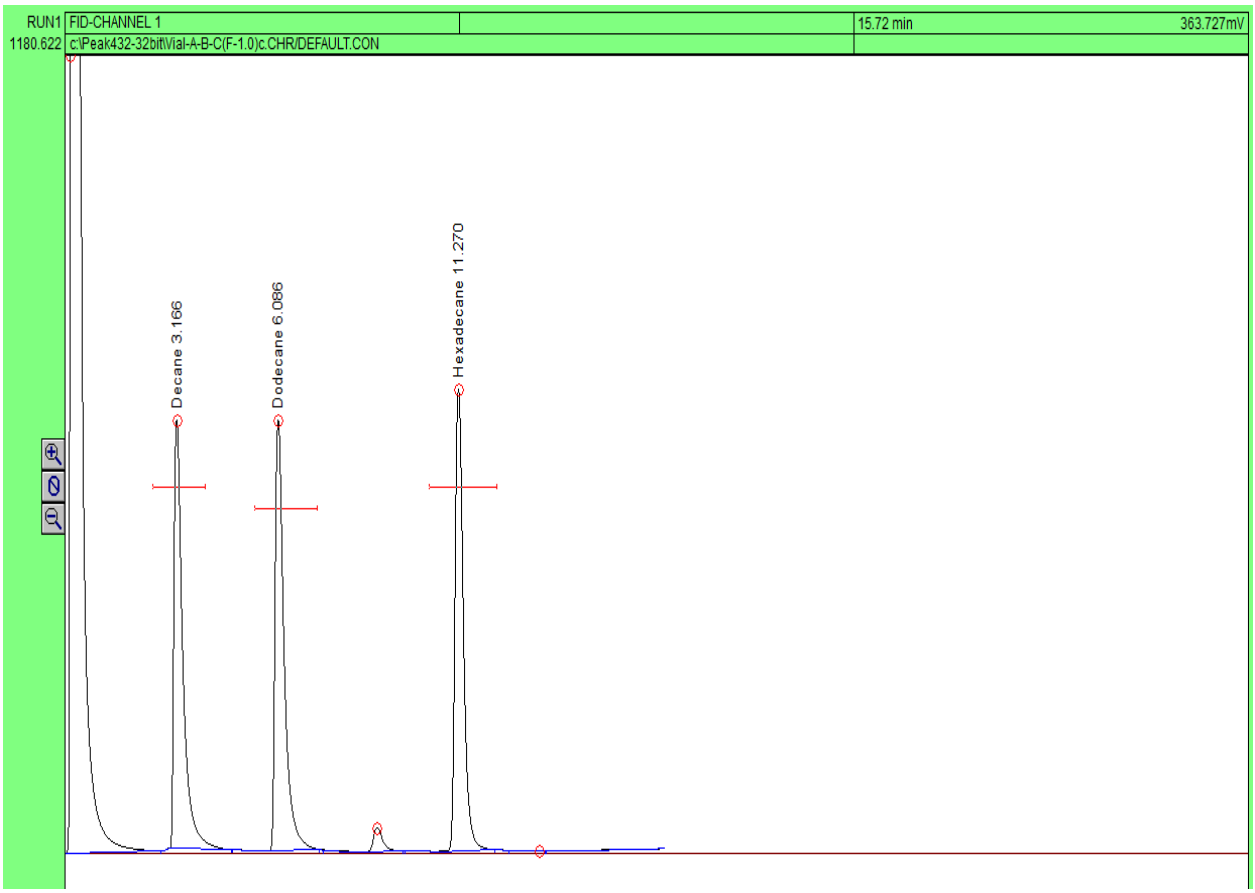

Figure 3-2, Gas chromatogram from peak-simple software

Table 3-2, Calibration of GC-FID with Decane, Dodecane and Hexadecane-Set 1

Parameters	**Decane**	**Dodecane**	**Hexadecane**
Density @ 20°C (g/cm^3)	0.73005	0.74869	0.77344
Molecular Weight (g/mol)	142.28	170.34	226.45
Actual Mass Used (g)	7.3005E-03	7.4869E-03	7.7344E-03
Actual Moles Used (mol)	5.1311E-05	4.3953E-05	3.4155E-05
Area @ 0.5µl (millivolts.sec)	5330.292	5271.9172	5076.6517
Moles @ 0.5µl (mol)	2.5630E-09	2.1954E-09	1.7060E-09
Area/Moles	2.0797E+12	2.4013E+12	2.9757E+12
Area/Moles Ratio	1.0000E+00	1.1546E+00	1.4308E+00
Density @ 20°C (g/cm^3)	0.73005	0.74869	0.77344
Molecular Weight (g/mol)	142.28	170.34	226.45
Actual Mass Used (g)	7.3005E-03	7.4869E-03	7.7344E-03
Actual Moles Used (mol)	5.1311E-05	4.3953E-05	3.4155E-05
Area @ 0.5µl (millivolts.sec)	5170.0742	5275.0982	5078.2422
Moles @ 0.5µl (mol)	2.5630E-09	2.1954E-09	1.7060E-09
Area/Moles	2.0172E+12	2.4028E+12	2.9766E+12
Area/Moles Ratio	1.0000E+00	1.1911E+00	1.4756E+00
Density @ 20°C (g/cm^3)	0.73005	0.74869	0.77344
Molecular Weight (g/mol)	142.28	170.34	226.45
Actual Mass Used (g)	7.3005E-03	7.4869E-03	7.7344E-03
Actual Moles Used (mol)	5.1311E-05	4.3953E-05	3.4155E-05
Area @ 0.5µl (millivolts.sec)	5222.5862	5125.4936	5174.0436
Moles @ 0.5µl (mol)	2.5630E-09	2.1954E-09	1.7060E-09
Area/Mass	2.0377E+12	2.3346E+12	3.0328E+12
Area/Moles Ratio	1.0000E+00	1.1457E+00	1.4883E+00
Density @ 20°C (g/cm^3)	0.73005	0.74869	0.77344
Molecular Weight (g/mol)	142.28	170.34	226.45
Actual Mass Used (g)	7.3005E-03	7.4869E-03	7.7344E-03
Actual Moles Used (mol)	5.1311E-05	4.3953E-05	3.4155E-05
Area @ 1.0µl (millivolts.sec)	10750.2466	10912.0582	10373.0282
Moles @ 1.0µl (mol)	5.1260E-09	4.3909E-09	3.4121E-09
Area/Mole	2.0972E+12	2.4852E+12	3.0401E+12
Area/Moles Ratio	1.0000E+00	1.1850E+00	1.4496E+00

Cont. of Table 3-2, Calibration of GC-FID with Decane, Dodecane and Hexadecane-Set 1

Parameters	**Decane**	**Dodecane**	**Hexadecane**
Density @ 20°C (g/cm^3)	0.73005	0.74869	0.77344
Molecular Weight (g/mol)	142.28	170.34	226.45
Actual Mass Used (g)	7.3005E-03	7.4869E-03	7.7344E-03
Actual Moles Used (mol)	5.1311E-05	4.3953E-05	3.4155E-05
Area @ 1.0µl (millivolts.sec)	10428.4862	10923.22	10714.7204
Moles @ 1.0µl (mol)	5.1260E-09	4.3909E-09	3.4121E-09
Area/Mole	2.0344E+12	2.4877E+12	3.1402E+12
Area/Moles Ratio	1.0000E+00	1.2228E+00	1.5435E+00
Density @ 20°C (g/cm^3)	0.73005	0.74869	0.77344
Molecular Weight (g/mol)	142.28	170.34	226.45
Actual Mass Used (g)	7.3005E-03	7.4869E-03	7.7344E-03
Actual Moles Used (mol)	5.1311E-05	4.3953E-05	3.4155E-05
Area @ 1.0µl (millivolts.sec)	10512.0472	10962.682	10390.7906
Moles @ 1.0µl (mol)	5.1260E-09	4.3909E-09	3.4121E-09
Area/Mole	2.0507E+12	2.4967E+12	3.0453E+12
Area/Moles Ratio	1.0000E+00	1.2175E+00	1.4850E+00

Table 3-3, Calibration of GC-FID with Decane, Dodecane and Hexadecane-Set 2

Parameters	Decane	Dodecane	Hexadecane
Density @ 20°C (g/cm^3)	0.73005	0.74869	0.77344
Molecular Weight (g/mol)	142.28	170.34	226.45
Actual Mass Used (g)	7.3005E-03	7.4869E-03	7.7344E-03
Actual Moles Used (mol)	5.1311E-05	4.3953E-05	3.4155E-05
Area @ 0.5µl	5161.077	5267.7066	5010.4024
Moles @ 0.5µl (mol)	2.5630E-09	2.1954E-09	1.7060E-09
Area/Moles	2.0137E+12	2.3994E+12	2.9369E+12
Area/Moles Ratio	1.0000E+00	1.1915E+00	1.4584E+00
Density @ 20°C (g/cm^3)	0.73005	0.74869	0.77344
Molecular Weight (g/mol)	142.28	170.34	226.45
Actual Mass Used (g)	7.3005E-03	7.4869E-03	7.7344E-03
Actual Moles Used (mol)	5.1311E-05	4.3953E-05	3.4155E-05
Area @ 0.5µl	5057.6654	5283.5334	5127.59
Moles @ 0.5µl (mol)	2.5630E-09	2.1954E-09	1.7060E-09
Area/Moles	1.9734E+12	2.4066E+12	3.0055E+12
Area/Moles Ratio	1.0000E+00	1.2195E+00	1.5231E+00
Density @ 20°C (g/cm^3)	0.73005	0.74869	0.77344
Molecular Weight (g/mol)	142.28	170.34	226.45
Actual Mass Used (g)	7.3005E-03	7.4869E-03	7.7344E-03
Actual Moles Used (mol)	5.1311E-05	4.3953E-05	3.4155E-05
Area @ 0.5µl	5021.6446	5366.218	5009.552
Moles @ 0.5µl (mol)	2.5630E-09	2.1954E-09	1.7060E-09
Area/Moles	1.9593E+12	2.4443E+12	2.9364E+12
Area/Moles Ratio	1.0000E+00	1.2475E+00	1.4987E+00
Density @ 20°C (g/cm^3)	0.73005	0.74869	0.77344
Molecular Weight (g/mol)	142.28	170.34	226.45
Actual Mass Used (g)	7.3005E-03	7.4869E-03	7.7344E-03
Actual Moles Used (mol)	5.1311E-05	4.3953E-05	3.4155E-05
Area @ 1.0µl	10883.5672	10761.7012	10203.0464
Moles @ 1.0µl (mol)	5.1260E-09	4.3909E-09	3.4121E-09
Area/Mole	2.1232E+12	2.4509E+12	2.9903E+12
Area/Moles Ratio	1.0000E+00	1.1543E+00	1.4084E+00

Cont. of Table 3-3, Calibration of GC-FID with Decane, Dodecane and Hexadecane-Set 2

Parameters	Decane	Dodecane	Hexadecane
Density @ 20^{o}C (g/cm^{3})	0.73005	0.74869	0.77344
Molecular Weight (g/mol)	142.28	170.34	226.45
Actual Mass Used (g)	7.3005E-03	7.4869E-03	7.7344E-03
Actual Moles Used (mol)	5.1311E-05	4.3953E-05	3.4155E-05
Area @ 1.0µl	10387.4142	10574.37	10346.5046
Moles @ 1.0µl (mol)	5.1260E-09	4.3909E-09	3.4121E-09
Area/Mole	2.0264E+12	2.4083E+12	3.0323E+12
Area/Moles Ratio	1.0000E+00	1.1884E+00	1.4964E+00
Density @ 20^{o}C (g/cm^{3})	0.73005	0.74869	0.77344
Molecular Weight (g/mol)	142.28	170.34	226.45
Actual Mass Used (g)	7.3005E-03	7.4869E-03	7.7344E-03
Actual Moles Used (mol)	5.1311E-05	4.3953E-05	3.4155E-05
Area @ 1.0µl	10563.0684	10801.278	10416.7806
Moles @ 1.0µl (mol)	5.1260E-09	4.3909E-09	3.4121E-09
Area/Mole	2.0607E+12	2.4599E+12	3.0529E+12
Area/Moles Ratio	1.0000E+00	1.1937E+00	1.4815E+00

The two different set of calibration values were obtained from two different 1000ppm standard solutions prepared by using the method stated above. The average calibration constant (Area/Mole) for the two set of tables (table 3-2 and table 3-3) was calculated as shown in table 3-4 and used for calculating the mole fractions of solutes in a solution. The overall mean calibration constant (Area/Mole) was used to determine the mole fractions of any solution whose concentration is unknown. To find the constituents of any solution, 1.0µl of that solution should be diluted with 1ml of hexane to form 1000ppm of solution and then injected into the GC to obtain the peak areas of each component. The obtained peaks from peak-simple software for each component are divided by their corresponding calibration constant to get the moles of each component injected. The mole fraction can then be calculated from the total moles.

Table 3-4, Calibration of GC-FID with Decane, Dodecane and Hexadecane

Calibration Set-1			
Parameters	Decane	Dodecane	Hexadecane
Mean (Area/Mole)	2.05284E+12	2.43471E+12	3.03511E+12
Calibration Set-2			
Parameters	Decane	Dodecane	Hexadecane
Mean (Area/Mole)	2.02612E+12	2.42823E+12	2.99237E+12
Overall Mean (Area/Mole)	**2.0395E+12**	**2.431E+12**	**3.0137E+12**

3.3 Experimental Procedure

The experiment procedure was carried out in two separate parts. The first part involved cooling and freezing of liquid samples in environmental chamber and withdrawing liquid samples at regular time interval. The second part involved the injection of liquid samples into the GC-FID to determine the compositions of the sample.

The amount of chemical used varied depending on whether a pure chemical or mixture of chemical is used. Firstly, pure dodecane is run in the experimental setup to measure the melting and freezing temperature profile and compared with literature data. This was done to ensure that the experimental procedure works well and also to get acquainted in running the experiment to be able to produce good results for the various mixtures which have no literature data available.

3.3.1 Experimental Procedure for Pure Dodecane: 100ml of pure dodecane is put in the test cell and placed on the retort stand and placed in the environmental chamber. From literature, the freezing point (T_f) of dodecane is 263.6 K (-9.55^{o}C) and based on that, the following cooling and freezing profile was developed.

Freezing Profile:

- The chamber was ramped from its initial temperature (24^{o}C) at 0.5^{o}C/min to -5^{o}C.

- From -5°C to -25°C, a different ramping rate of 0.1°C/min will be used since pure dodecane freezes at -9.55°C which makes it an area of interest with solid-liquid transition occurring within this temperature range.

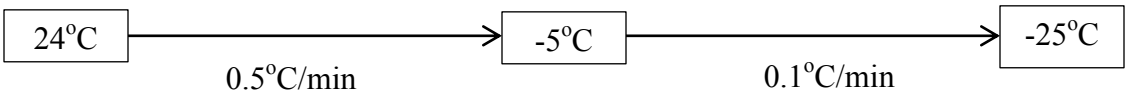

Melting Profile

- From -25°C to -5°C a ramping rate of 0.1°C/min was used to cover the solid-liquid transition range for pure dodecane.
- The last step was to move the temperature from -5°C to 24°C which was done with a ramping rate of 0.5°C/min.

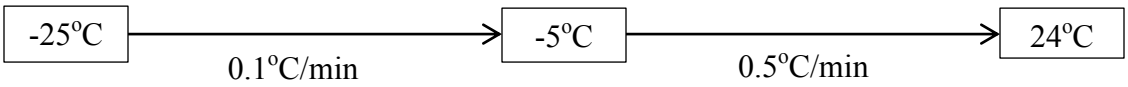

For the entire melting and freezing profile, the temperature reading of the thermocouple and environmental chamber was recorded at every two minutes interval.

3.3.2 Experimental Procedure for Mixture of Decane and Dodecane: A total volume of 150ml of dodecane and hexadecane mixture is put in a test cell and placed on the retort stand in the environmental chamber. Several different compositions of the binary mixtures were prepared. The binary compositions varied from pure decane to pure dodecane. The ramping rate profile was designed as follows:

Freezing Profile:

- The chamber was ramped from its initial temperature (24°C) at 0.5°C/min to -5°C.

- A reduced ramping rate of 0.1°C/min is set from -5°C to -35°C because solid-liquid transition is presumed to occur in this temperature range. The temperature is held at -35°C for 15 minutes and then ramped into the melting profile.

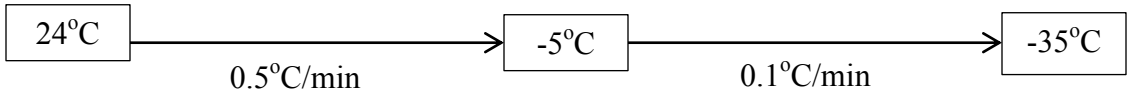

Melting Profile:

- From -35°C to -5°C, a ramping rate of 0.1°C is used to be able to record a detailed temperature behavior of the mixture in its solid-liquid transition.
- The last step was to move the temperature from -5°C to 24°C which was done at a rate of 0.5°C/min.

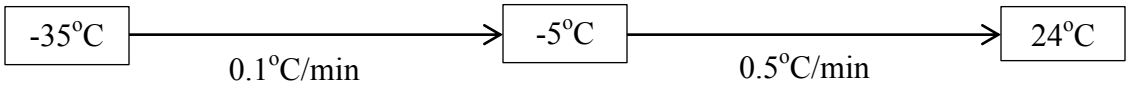

The temperature readings for the environmental chamber and thermocouple immersed in the test cell is recorded at every 2 minute. 1.0µl of each liquid sample withdrawn was diluted with 1.0ml of solvent (hexane) to form 1000ppm solution of the solutes to obtain good data from the GC. This was done to prevent the truncation of peaks when high concentrations of solutes are injected into the GC.

The liquid samples were not withdrawn right from the onset of ramping. The first three liquid samples were withdrawn when the sample temperature displayed the various temperature values: -8°C, -9°C and -10°C. The subsequent temperature readings were taken at every 2°C temperature rise until no liquid sample could be withdrawn. 1.0µl of the liquid is withdrawn from 1/8 inch T-shaped fitting with a 1µl syringe and diluted in a 1ml of hexane contained in a 2ml vial. The T-shaped tube fitting has septum inserted in an outlet which the syringe pierces through when samples were taken. Before the liquid were withdrawn, a metering valve

connected after the T-shaped fitting is opened to remove the initial liquid filled in the tube. The valve is opened 180^{o} anticlockwise for about 20seconds and quickly closed before the liquid is withdrawn with the syringe. This is to ensure that the liquid withdraw is actually what is inside the test cell at a particular temperature. The metering valve is closed tightly before the liquid sample is withdrawn to minimize sample loss. The experimental results are shown in Chapter 4.

CHAPTER 4

Results

4.1 Freezing and Melting Curves for Pure Dodecane

The freezing and melting temperature profiles of pure dodecane were recorded. The two temperature profiles were recorded within a time interval of two minutes. This was done to ensure that the experimental procedure works well and also to get acquainted in running the experimental chamber to be able to produce good results for the various mixtures which have no literature data available. The figure 4-1 shows a graph of freezing and melting temperature profile against time for pure dodecane with the raw data in appendix A precisely table A-2 and A-3. From literature, dodecane is said to have a freezing point of -9.55^{o}C.

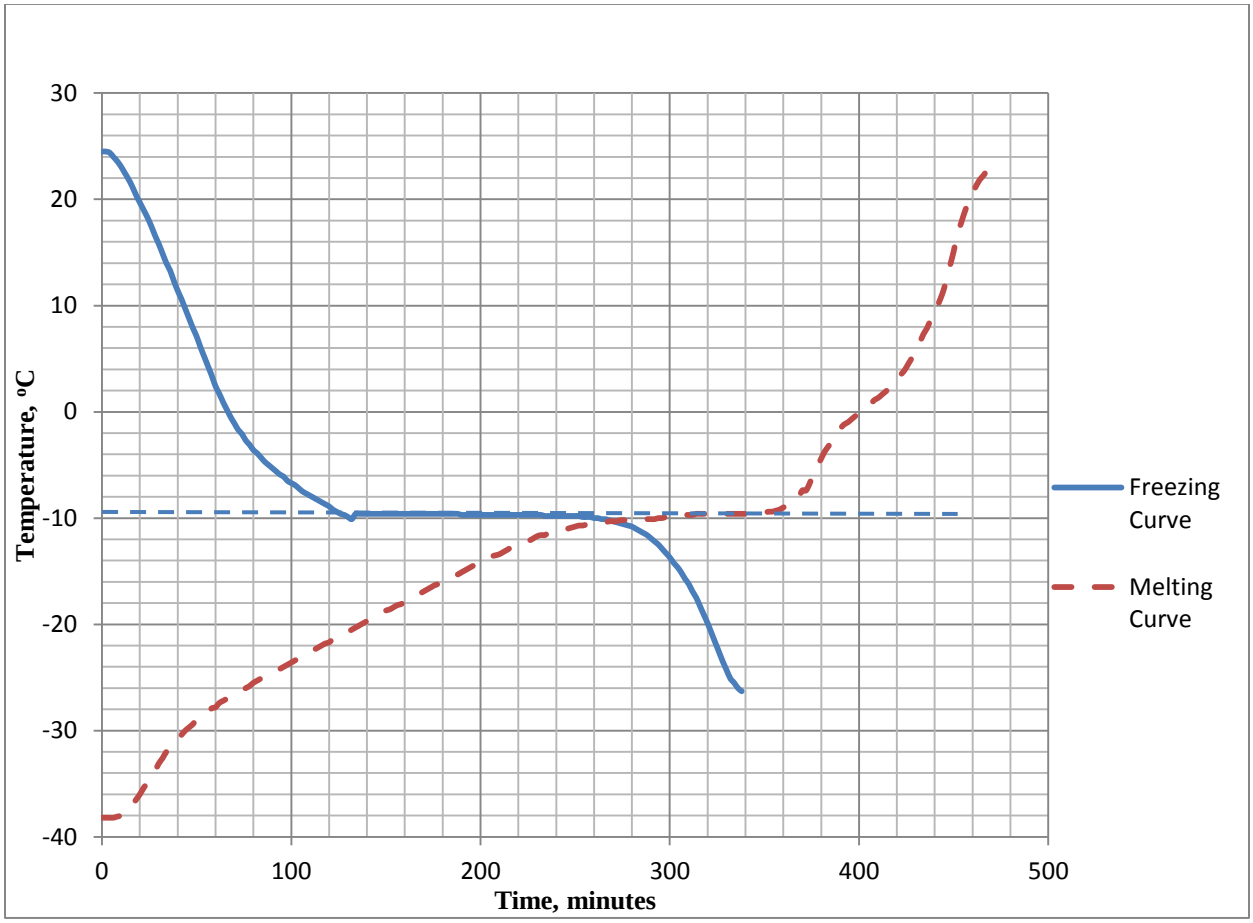

Figure 4-1, Freezing and melting temperature profile for pure dodecane

4.2 Freezing and Melting Curves for Pure Decane

The freezing and melting temperature profiles of pure dodecane were recorded. The two temperature profiles were recorded within a time interval of two minutes. Mohammed Ali recorded the temperature profile with the ramping method describe as follows. The temperature was ramped from the initial temperature of the chamber to -20°C with ramped rate of 0.8°C/min. A slow ramping rate of 0.1°C/min was used to move the temperature from -20°C to -40°C. The melting profile was then ramped from -40°C to -20°C with a ramping rate of 0.1°C/min. The last step of the melting was ramped from -20°C to 24°C with ramped rate of 0.8°C/min. The pure decane temperature profile is shown in the figure 4-2 below.

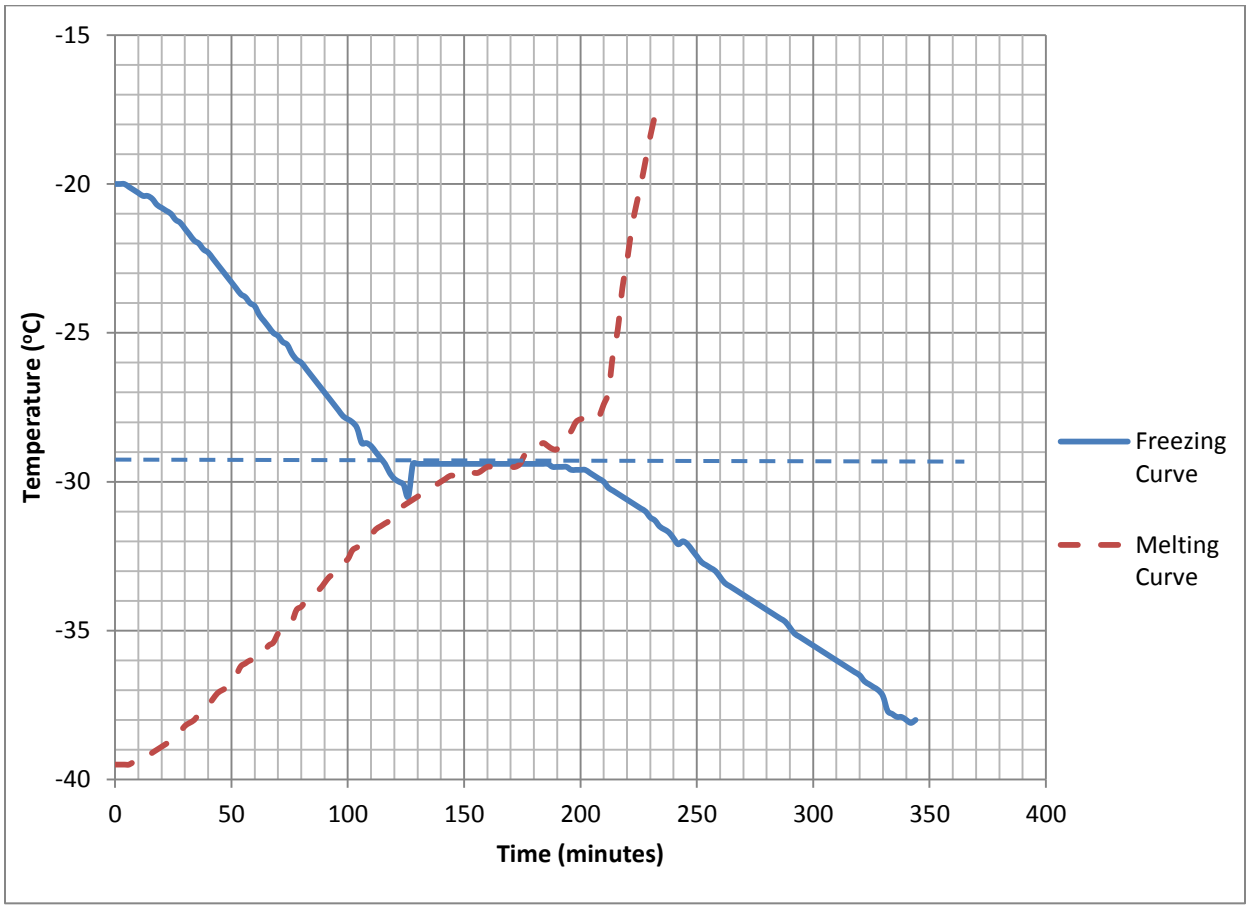

Figure 4-2, Temperature profile for pure decane (experiment by Mohammed Ali)

4.3 Freezing and Melting Curves for Mixtures of Decane (1) and Dodecane (2)

Several mixtures of decane and dodecane with different mole fractions of decane (1) and dodecane (2) were prepared for the temperature profile experiment. The temperature profile was designed as follows: For the freezing cycle, the chamber was generally ramped from its initial temperature (24^{o}C) to -5 with a ramping rate of 0.5^{o}C and had the ramped rate slowed down to 0.1^{o}C/min from -5^{o}C to -50^{o}C. The melting profile was then ramped from -50^{o}C to -5^{o}C with a ramping rate of 0.1^{o}C/min. The last step of the melting was ramped from -5^{o}C to 24^{o}C with ramped rate of 0.5^{o}C/min. The mixture of decane and dodecane temperature profile is shown in the Figures below. The horizontal short dashes lines indicate the solid liquid transition temperatures of the temperature profile diagrams.

In the first binary temperature profile experiment, this was the mixture of decane (1) and dodecane (2) with $x_1 = 0.84$, liquid samples withdrawn from the metal whiles freezing and melting at specific temperatures showed no change in composition from its initial composition placed in the metal cell from the onset of the experiment.

Liquid samples were also withdrawn when the experiment was run with a mixture of decane (1) and dodecane (2) with $x_1 = 0.15$, and that also showed no change in composition from its initial composition. Liquid samples were not withdrawn when the temperature profile for the remaining binary mixture experiment were carried out. Because we had an idea of the temperature range where the solid-liquid transition will occur, the temperature was ramped at 0.8^{o}C/min to a temperature closer to the transition temperature of the mixture and then ramped at 0.1^{o}C/min within the expected solid-liquid transition temperature range.

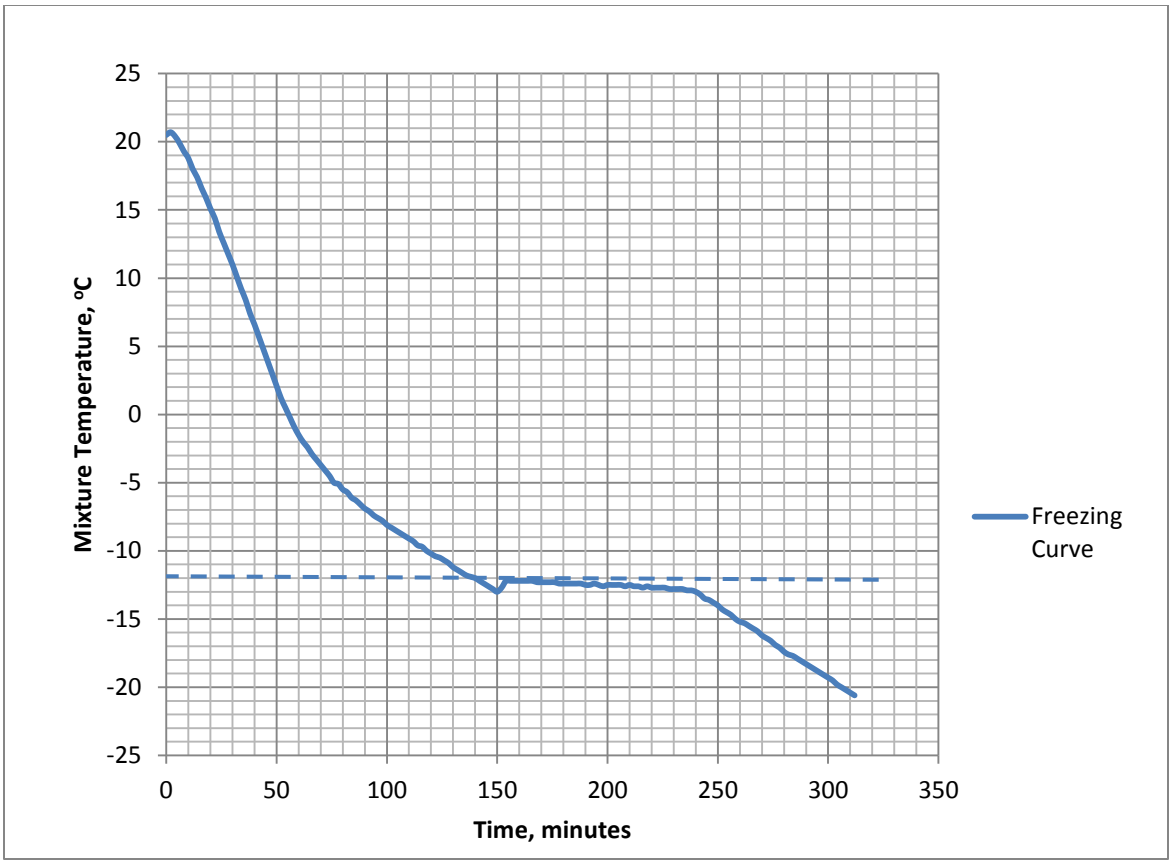

Figure 4-3, Temperature profile for mixture of decane-dodecane with $x_1 = 0.15$

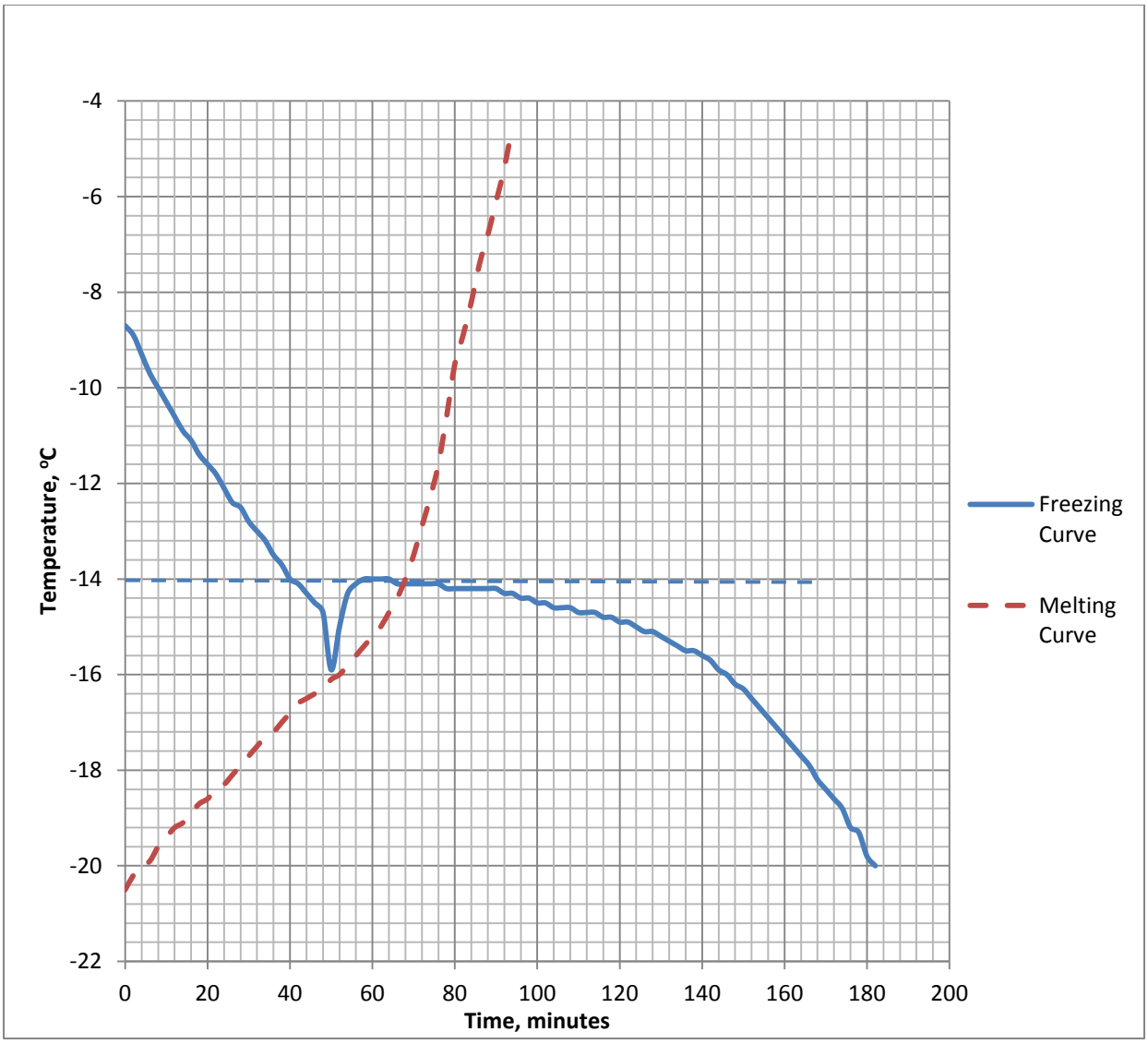

Figure 4-4, Temperature profile for mixture of decane-dodecane with $x_1 = 0.25$

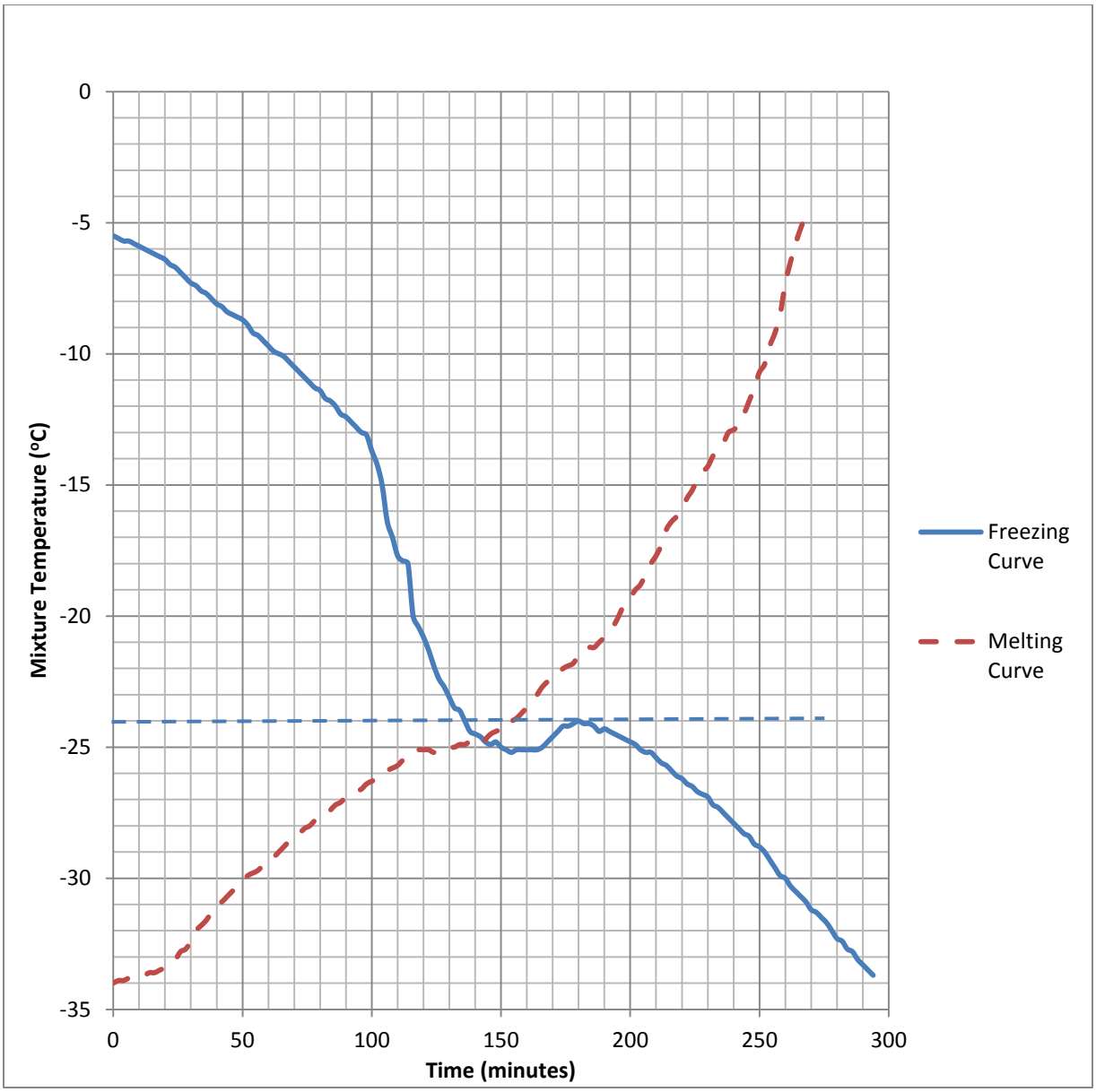

Figure 4-5, Temperature profile for mixture of decane-dodecane with $x_1 = 0.54$ (experiment by Mohammed Ali)

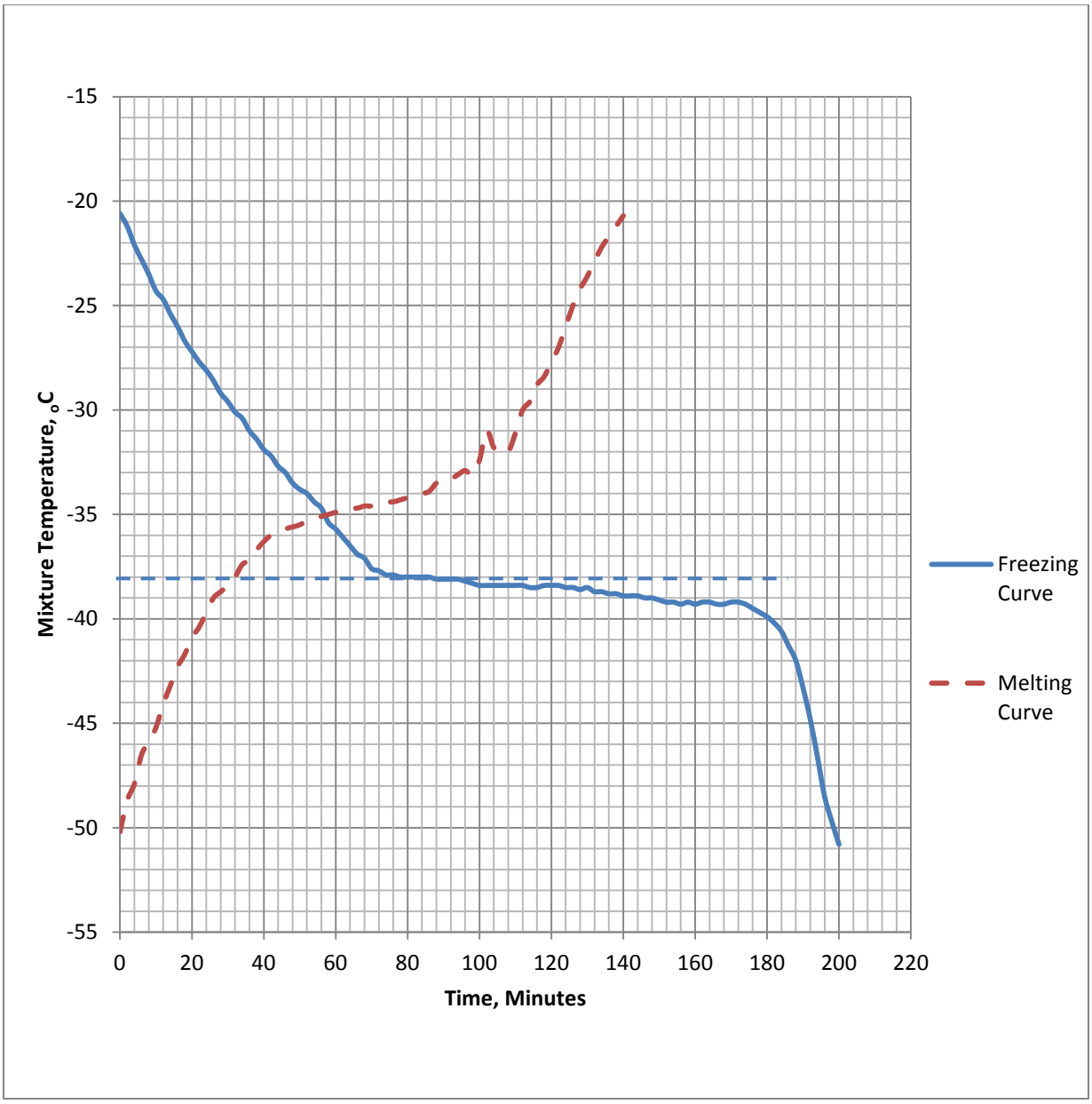

Figure 4-6, Temperature profile for mixture of decane-dodecane with $x_1 = 0.80$

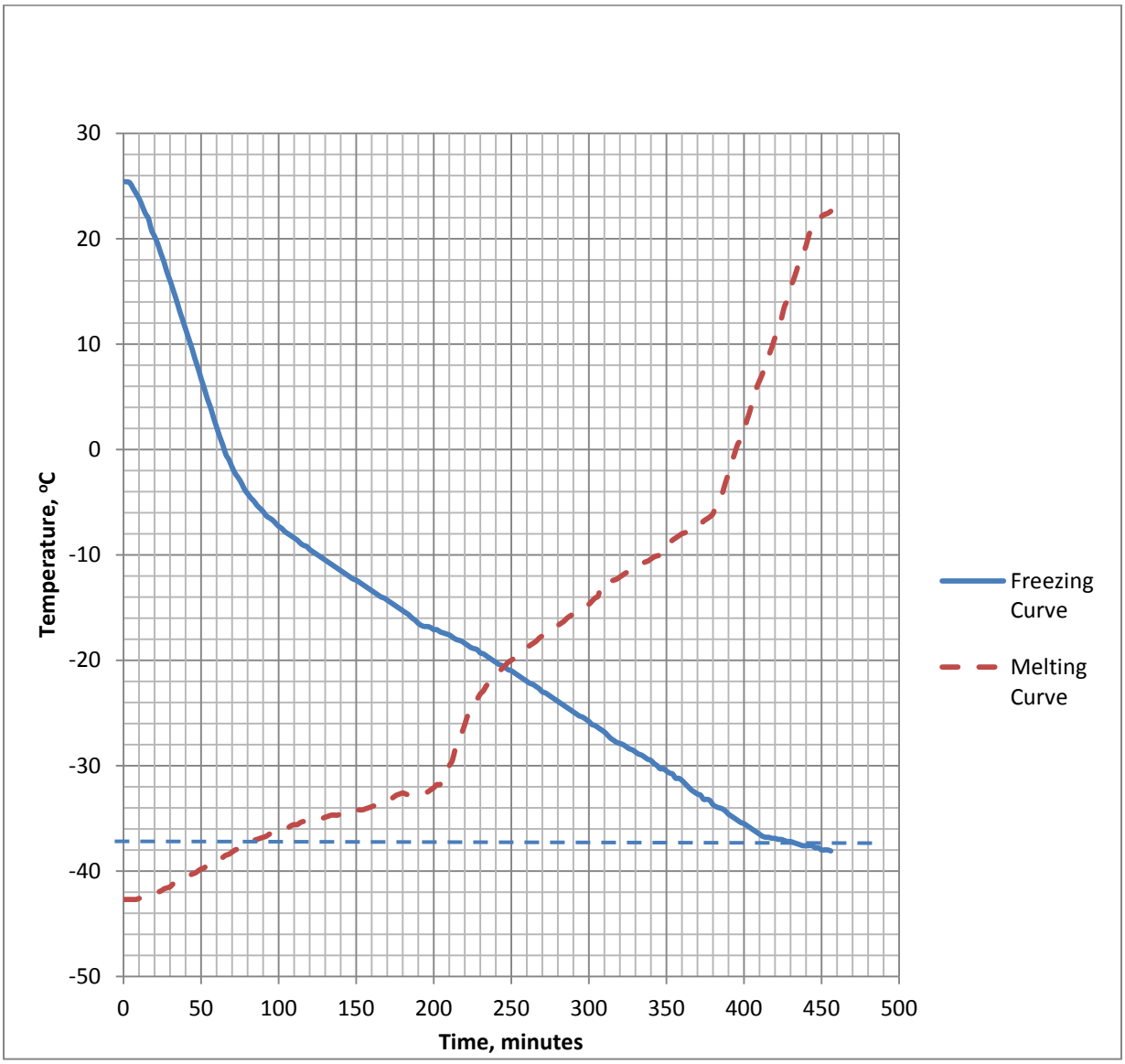

Figure 4-7, Temperature profile for mixture of decane-dodecane with $x_1 = 0.84$

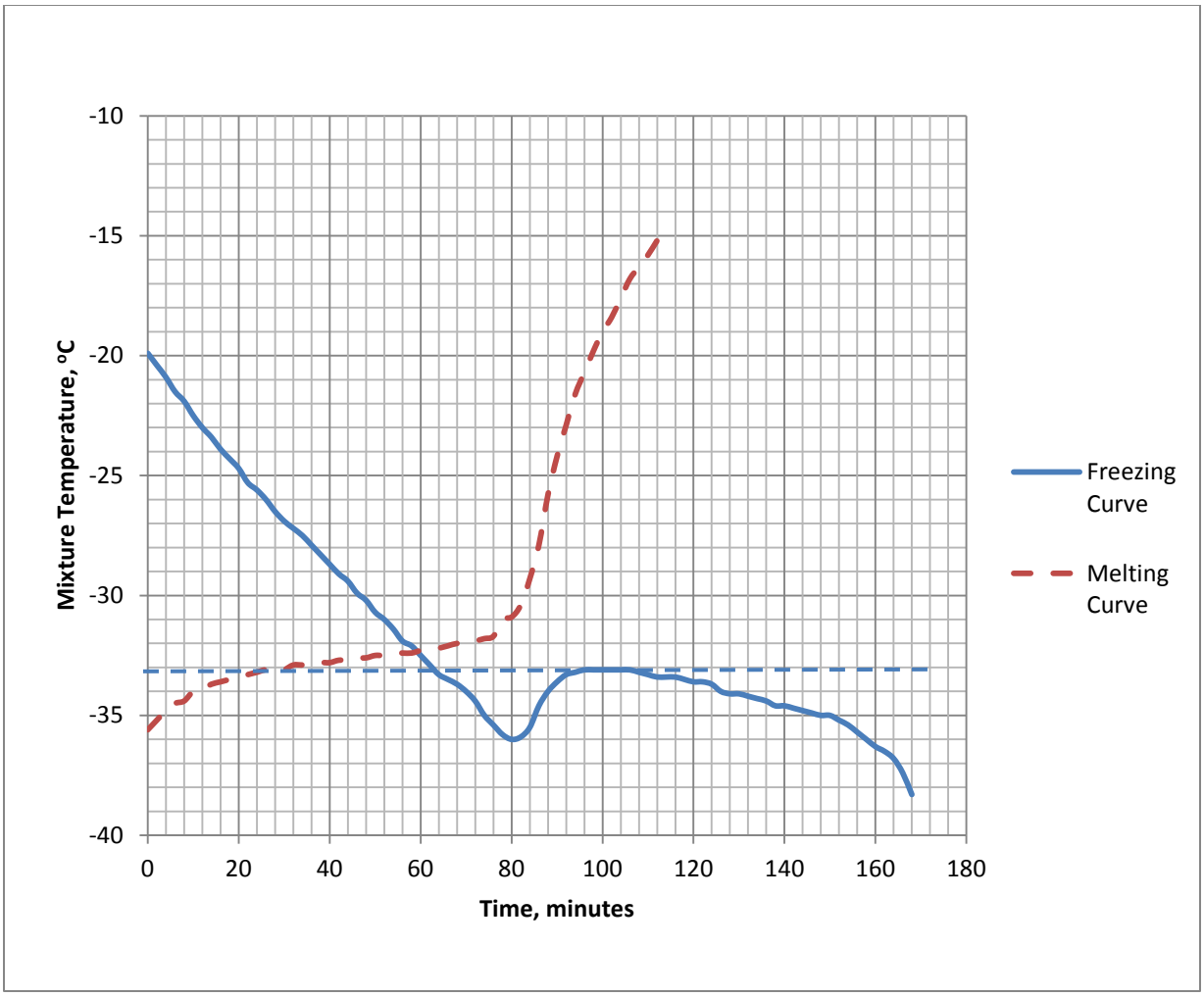

Figure 4-8, Temperature profile for mixture of decane-dodecane with $x_1 = 0.90$

4.4 Freezing and Melting Curves for a Mixture of Decane, Dodecane and Hexadecane

A mixture of equal volume of decane, dodecane and hexadecane with 50ml of decane, 50ml of dodecane and 50ml of hexadecane was prepared for the temperature profile experiment. The temperature profile was designed as follows: For the freezing cycle, the chamber was slowly ramped from its initial temperature (24°C) to 15 with a ramping rate of 0.1°C and had the ramped rate increased to 1°C/min from 15°C to 0°C. The ramping rate was again decreased to 0.1°C/min from 0°C to -35°C. The melting profile was then ramped from -35°C to 24°C with a ramping rate of 0.1°C/min. The mixture of decane, dodecane and hexadecane temperature profile is shown in

the Figure 4.9 below. Further work will be carried on ternary mixture to obtain their solid-liquid equilibrium data.

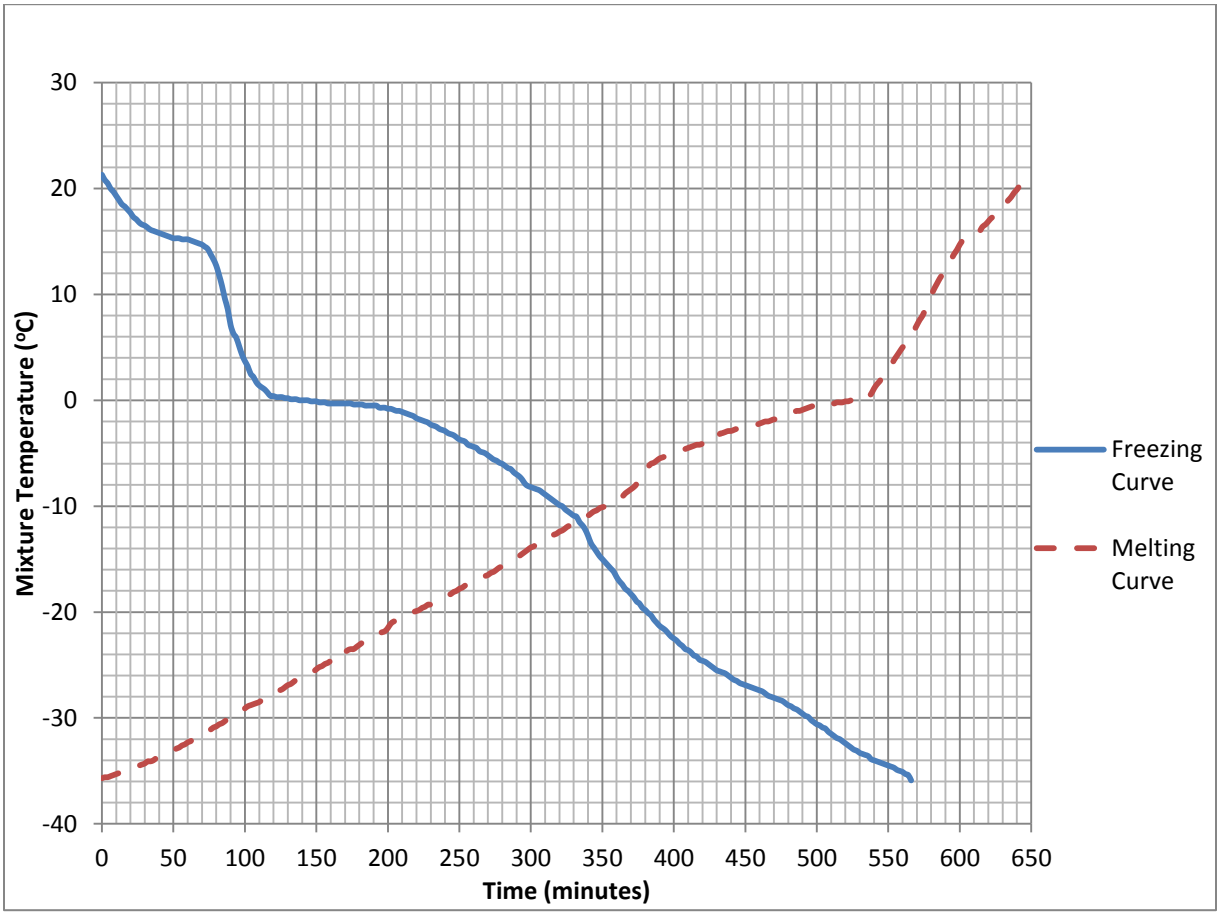

Figure 4-9, Temperature profile for mixture of equal volume of decane, dodecane and hexadecane (experiment by Mohammed Ali)

4.5 Freezing and Melting Curves for Mixtures of Decane (1) and Dodecane (2)

The freezing and melting temperature profiles of binary system of decane and dodecane were recorded as well as the composition of the liquid sample at various temperatures was also analyzed with a gas chromatograph. Six binary compositions of decane and dodecane were prepared and analyzed. The table 4-1 shows the mole fraction of the various binary systems prepared.

Table 4-1, Sample binary systems for decane and dodecane

	Mole Fraction		Freezing/Melting Temperature ^{o}C	Freezing/Melting Temperature ^{o}K
Sample	Decane	Dodecane		
1	0	1	-9.55	263.6
2	0.1518	0.8482	-12	261.15
3	0.247	0.753	-14	259.15
4	0.5386	0.4614	-24	249.15
5	0.8001	0.1999	-38	235.15
6	0.8357	0.1646	-37	236.15
7	0.8988	0.1012	-33	240.15
8	1	0	-29.5	243.65

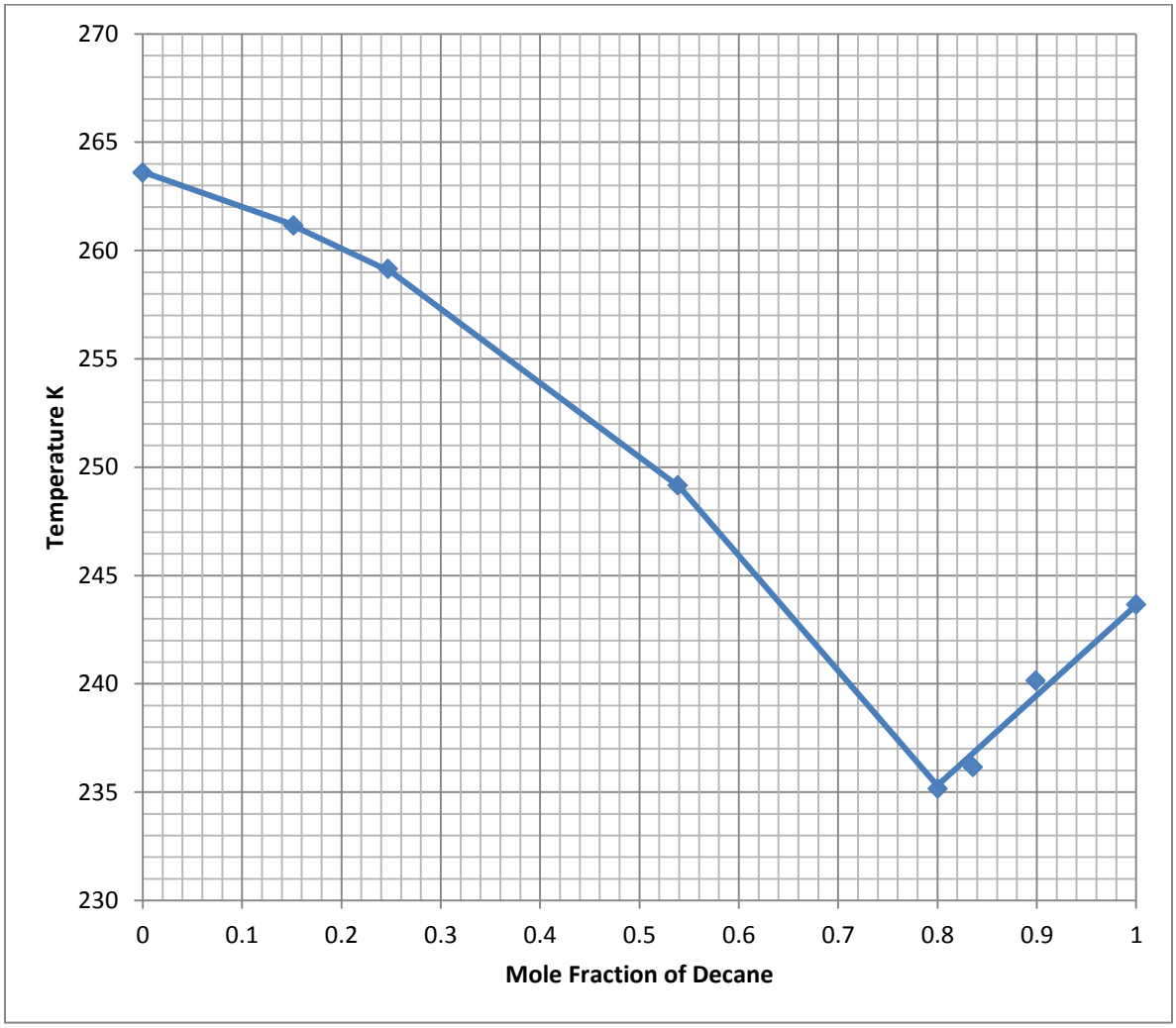

Figure 4-10, Binary phase diagram for Decane and Dodecane

CHAPTER 5

Discussion and Future Research

5.1 Freezing and Melting Curves for Pure Dodecane

Figure 4-1, shows the temperature profile of freezing and melting for pure dodecane. The time-temperature freezing curve for pure dodecane shows a steep change in slope from the onset of freezing until the temperature get closed -10^{o}C. At -10^{o}C, the profile shows a constant temperature (T = -10^{o}C) for a period of time with both freezing and melting profiles. The temperature then steeply decreases until it hits -25^{o}C which ends the freezing cycle of dodecane

The initial drastic change in slope of the freezing curve signifies the loss of sensible heat from the sample as it approaches it freezing point. The section which shows a constant temperature for a period of time signifies the change in phase of the liquid sample from liquid to solid. Before the constant temperature period, the freezing profile experienced and sharp drop and rise in temperature. This phenomenon signifies the sub-cooling of the liquid before freezing. Subcooling is when the liquid existing at a temperature falls below its normal saturation temperature (freezing temperature). The solid-liquid transition which takes place involves the loss of latent heat from the sample. From the data recorded in Table A-2 in Appendix A, it shows a value -9.6^{o}C as the freezing point of dodecane, which is close to the literature value of -9.55^{o}C. The liquid molecules at this stage loose its energy and become closely packed. As shown in Table A-1 in Appendix A, the pure dodecane changes from the liquid phase to triclinic solid phase, where the chains make an angle of about 73^{o} with the end group planes, with its rotation greatly restricted. The final steep change in slope for the freezing curve also signifies the loss of sensible heat after the liquid has completely transited into triclinic phase. The same temperature profile behavior is repeated in the melting curve.

5.2 Freezing and Melting Curves of Decane, Dodecane and Hexadecane

Several different pure binary samples were prepared for this particular experiment. The samples were pure dodecane, binary mixture of decane and dodecane with different mole fractions and ternary mixture of decane, dodecane and hexadecane also in equal volumes.

The time-temperature profile for pure decane shows a constant temperature T=-29.4^{o}C which corresponds with the freezing point of pure decane in literature as shown in Figure 4-2. The time-temperature profile of the mixture (decane+dodecane+hexadecane) shows a change in slope at T=-0.3^{o}C. It then shows another change in slope at 15^{o}C with a few gradual increase in temperature before it increases steadily again as shown in Figure 4-4.

5.3 Freezing and Melting for Binary Mixture of Decane and Dodecane

The time-temperature profile for the different mole fractions of the binary mixture of decane and dodecane shows a constant temperature or reduce in slope in the melting and freezing curve. A reduce in slope in the temperature or a constant temperature signifies a solid-liquid transition. The Figure 4-3 – 4.7 shows the temperature profile for the binary system. From these Figures, it shows that the binary system of decane and dodecane have different solid-liquid transition temperature base on their mole fractions.

Decane and dodecane are straight chain even normal paraffins with isomorphic structures in the solid state. From table A-1 in appendix, both decane and dodecane have the same solid phase structure. Both pure decane and dodecane have liquid-solid phase transition from liquid to triclinic solid phase. Since decane and dodecane are even paraffins, they form solid solution when frozen together. The binary mixture of decane and dodecane when frozen together form one unique crystal structure with no different phases which makes it to be considered as a solid solution. The individual pure decane and dodecane do not crystallize separately. This explains

why the liquid samples withdrawn from the metal cell whiles freezing or melting showed no different composition from its initial sample, because both components crystallize together as shown in Table B-12 in Appendix-B

Figure 4-10 shows a binary phase diagram for decane and dodecane. This phase diagram displays the solid-liquid transition temperature for the mixture of decane and dodecane at different mole fractions. From the diagram, it can be said that, the lowest temperature for solid-liquid transition for the binary mixture is 235.15K with mole fractions of 0.8001 decane and 0.1999 dodecane. This lowest temperature is called the eutectic temperature for the system.

Further work would be carried out in modeling the solid-liquid equilibrium of hydrocarbon mixtures. A theoretical model based on the local composition concept can be used to describe the solid-phase non-ideality which remains an obstacle in the modeling of solid-liquid and solid-solid equilibrium.

Finally, a reduced ramping rate will be used for the melting cycle of multicomponent system since the melting curve for the above temperature profile diagram did not give a detailed solid-liquid transition temperature region. Other experimental work would be carried on different binary and ternary phase system to develop more phase diagrams to compare the performance of developed models with the experimental data

References

1. Broadhurst, M.G., J. Res. Natl. Bur. Stand., 1962. **66A**: p. 241.
2. Wilson, G.M., *Vapor-liquid equilibrium. XI. A new expression for the excess free energy of mixing.* J. Am. Chem. Soc., 1964. **86**: p. 127-130.
3. Coutinho, J.A., K. Knudsen, S.I. Andersen, and E.H. Stenby, *A local composition model for paraffinic solid solutions.* Chemical engineering science, 1996. **51**(12): p. 3273-3282.
4. Milhet, M., J. Pauly, J.A.P. Coutinho, M. Dirand, and J.L. Daridon, *Liquid–solid equilibria under high pressure of tetradecane+pentadecane and tetradecane+hexadecane binary systems.* Fluid Phase Equilibria, 2005. **235**(2): p. 173-181.
5. Dorset, D.L., *Crystal structure of n-paraffin solid solutions-an electron diffraction study.* Macromolecules, 1985. **18**(11): p. 2158-2163.
6. Wu, Y., K. Liu, B.A. Bamgbade, and M.A. McHugh, *Investigation on the solidification of several pure cyclic and aromatic hydrocarbons at pressures to 300MPa.* Fuel, 2013. **111**(0): p. 75-80.
7. *Standard Test Method for Freezing point of Fuels (Automatic Phase Transition Method), ASTM Standard D5972.* American Society for Testing and Materials, 2010. **05**.
8. *Standard Test Method for Freezing Point of Aviation Fuels (Automatic Laser Method), ASTM Standard D7153, Book of Standards.* American Society for Testing and Materials, 2010. **05**.
9. *Standard Test Methods for Freezing Point of Aviation Fuels, ASTM Standard D2386, Book of Standards.* American Society for Testing and Materials, 2012. **06**.

10. Machado, J.J.B., T.W. de Loos, E. Christian Ihmels, K. Fischer, and J. Gmehling, *High pressure solid–solid and solid–liquid transition data for long chain alkanes.* The Journal of Chemical Thermodynamics, 2008. **40**(12): p. 1632-1637.

11. Domańska, U. and P. Morawski, *Solid + liquid equilibria of (n-alkane + cyclohexane) mixtures at high pressures.* Fluid Phase Equilibria, 2004. **218**(1): p. 57-68.

12. Morawski, P., J.A.P. Coutinho, and U. Domańska, *High pressure (solid+liquid) equilibria of n-alkane mixtures: experimental results, correlation and prediction.* Fluid Phase Equilibria, 2005. **230**(1–2): p. 72-80.

13. Tanaka, Y. and M. Kawakami, *Solid-liquid phase equilibria in binary (benzene, cyclohexane + n-tetradecane, n-hexadecane) systems at temperatures 230–323 K and pressures up to 120 MPa.* Fluid Phase Equilibria, 1996. **125**(1–2): p. 103-114.

14. Dirand, M., M. Bouroukba, A.-J. Briard, V. Chevallier, D. Petitjean, and J.-P. Corriou, *Temperatures and enthalpies of (solid+solid) and (solid+liquid) transitions of n-alkanes.* The Journal of Chemical Thermodynamics, 2002. **34**(8): p. 1255-1277.

15. Machado, J.J.B. and T.W. de Loos, *Liquid–vapour and solid–fluid equilibria for the system methane + triacontane at high temperature and high pressure.* Fluid Phase Equilibria, 2004. **222–223**(0): p. 261-267.

16. Flöter, E., T.W. de Loos, and J. de Swaan Arons, *High pressure solid-fluid and vapour-liquid equilibria in the system (methane + tetracosane).* Fluid Phase Equilibria, 1997. **127**(1–2): p. 129-146.

17. Domanska, U. and P. Morawski, *(Solid+liquid) equilibria of (n-alkanes+ethyl 1,1-dimethylpropyl ether).* The Journal of Chemical Thermodynamics, 2001. **33**(10): p. 1215-1226.

18. Khimeche, K., Y. Boumrah, M. Benziane, and A. Dahmani, *Solid–liquid equilibria and purity determination for binary n-alkane+naphthalene systems.* Thermochimica Acta, 2006. **444**(2): p. 166-172.

19. Yang, M., E. Terakawa, Y. Tanaka, T. Sotani, and S. Matsuo, *Solid–liquid phase equilibria in binary (1-octanol + n-alkane) mixtures under high pressure: Part 1. (1-Octanol + n-tetradecane or n-hexadecane) systems.* Fluid Phase Equilibria, 2002. **194–197**(0): p. 1119-1129.

20. Gregorowicz, J., *Phase behaviour in the vicinity of the three-phase solid–liquid–vapour line in asymmetric nonpolar systems at high pressures.* Fluid Phase Equilibria, 2006. **240**(1): p. 29-39.

21. Esmaeilzadeh, F., J.F. Kaljahi, and E. Ghanaei, *Investigation of different activity coefficient models in thermodynamic modeling of wax precipitation.* Fluid Phase Equilibria, 2006. **248**(1): p. 7-18.

22. Won, K.W., *Thermodynamics for solid solution-liquid-vapor equilibria: wax phase formation from heavy hydrocarbon mixtures.* Fluid Phase Equilibria, 1986. **30**(0): p. 265-279.

23. Pauly, J., C. Dauphin, and J.L. Daridon, Fluid Phase Equilib., 1998. **149**: p. 173.

24. Schou Pedersen, K., P. Skovborg, and H.P. Roenningsen, *Wax precipitation from North Sea crude oils. 4. Thermodynamic modeling.* Energy & Fuels, 1991. **5**(6): p. 924-932.

25. Ungerer, P., B. Faissat, C. Leibovici, H. Zhou, E. Behar, G. Moracchini, and J.P. Courcy, *High pressure-high temperature reservoir fluids: investigation of synthetic condensate gases containing a solid hydrocarbon.* Fluid Phase Equilibria, 1995. **111**(2): p. 287-311.

26. Ghanaei, E., F. Esmaeilzadeh, and J. Fathikalajahi, *High pressure phase equilibrium of wax: A new thermodynamic model.* Fuel, 2014. **117, Part A**(0): p. 900-909.

27. Coutinho, J.A.P., *Predictive UNIQUAC: A New Model for the Description of Multiphase Solid−Liquid Equilibria in Complex Hydrocarbon Mixtures.* Industrial & Engineering Chemistry Research, 1998. **37**(12): p. 4870-4875.

28. Won, K.W., *Thermodynamic calculation of cloud point temperatures and wax phase compositions of refined hydrocarbon mixtures.* Fluid Phase Equilibria, 1989. **53**(0): p. 377-396.

29. Coutinho, J.A.P., S.I. Andersen, and E.H. Stenby, *Evaluation of activity coefficient models in prediction of alkane solid-liquid equilibria.* Fluid Phase Equilibria, 1995. **103**(1): p. 23-39.

30. Coutinho, J.A.P. and E.H. Stenby, *Predictive Local Composition Models for Solid/Liquid Equilibrium in n-Alkane Systems: Wilson Equation for Multicomponent Systems.* Industrial & Engineering Chemistry Research, 1996. **35**(3): p. 918-925.

31. Coutinho, J.A.P. and V. Ruffier-Méray, *Experimental Measurements and Thermodynamic Modeling of Paraffinic Wax Formation in Undercooled Solutions.* Industrial & Engineering Chemistry Research, 1997. **36**(11): p. 4977-4983.

32. Pauly, J., J.-L. Daridon, J.A.P. Coutinho, N. Lindeloff, and S.I. Andersen, *Prediction of solid–fluid phase diagrams of light gases–heavy paraffin systems up to 200 MPa using an equation of state–GE model.* Fluid Phase Equilibria, 2000. **167**(2): p. 145-159.

33. Coutinho, J.A.P., *Predictive local composition models: NRTL and UNIQUAC and their application to model solid–liquid equilibrium of n-alkanes.* Fluid Phase Equilibria, 1999. **158–160**(0): p. 447-457.

34. Prausnitz, J.M., R.N. Lichtenthaler, and E.G. de Azevedo, *Molecular thermodynamics of fluid-phase equilibria*. 3rd ed. 1998: Pearson Education.

35. Gmehling, J.G., T.F. Anderson, and J.M. Prausnitz, *Solid-Liquid Equilibria Using UNIFAC.* Industrial & Engineering Chemistry Fundamentals, 1978. **17**(4): p. 269-273.

36. Coutinho, J.A.P., S.I. Andersen, and E.H. Stenby, *Solid-liquid equilibrium of n-alkanes using the chain delta lattice parameter model.* Fluid Phase Equilibria, 1996. **117**(1–2): p. 138-145.

37. Yang, M., T. Narita, Y. Tanaka, T. Sotani, and S. Matsuo, *Solid–liquid phase equilibria in binary (1-octanol + n-alkane) mixtures under high-pressure: Part 2. (1-Octanol + n-octane, n-dodecane) systems.* Fluid Phase Equilibria, 2003. **204**(1): p. 55-64.

38. González, J.A., M. Zawadzki, and U. Domanska, *Thermodynamics of mixtures containing polycyclic aromatic hydrocarbons.* Journal of Molecular Liquids, 2008. **143**(2–3): p. 134-140.

39. Sekhar, G.C., P. Venkatesu, T. Hofman, and M.V.P. Rao, *Solid–liquid equilibria of long chain n-alkanes (C18–C28) in N,N-dimethylacetamide.* Fluid Phase Equilibria, 2002. **201**(2): p. 219-231.

40. van der Kooi, H.J., E. Flöter, and T.W.d. Loos, *High-pressure phase equilibria of {(1−x)CH4+xCH3(CH2)18CH3}.* The Journal of Chemical Thermodynamics, 1995. **27**(8): p. 847-861.

41. Parks, G.S., H.M. Huffman, and S.B. Thomas, *THERMAL DATA ON ORGANIC COMPOUNDS. VI. THE HEAT CAPACITIES, ENTROPIES AND FREE ENERGIES OF SOME SATURATED, NON-BENZENOID HYDROCARBONS1.* Journal of the American Chemical Society, 1930. **52**(3): p. 1032-1041.

42. Huffman, H.M., G.S. Parks, and M. Barmore, *Thermal data on organic compounds. X. Further studies on the heat capacities, entropies and free energies of hydrocarbons.* Journal of the American Chemical Society, 1931. **53**(10): p. 3876-3888.

43. Segovia, J.J., D. Vega-Maza, C.R. Chamorro, and M.C. Martín, *High-pressure isobaric heat capacities using a new flow calorimeter.* The Journal of Supercritical Fluids, 2008. **46**(3): p. 258-264.

44. Finke, H., M. Gross, G. Waddington, and H. Huffman, *Low-temperature thermal data for the nine normal paraffin hydrocarbons from octane to hexadecane.* Journal of the American Chemical Society, 1954. **76**(2): p. 333-341.

45. Aston, J.G., G.J. Szasz, and H.L. Fink, *The Heat Capacity and Entropy, Heats of Transition, Fusion and Vaporization and the Vapor Pressures of Cyclohexane. The Vibrational Frequencies of Alicyclic Ring Systems1.* Journal of the American Chemical Society, 1943. **65**(6): p. 1135-1139.

46. Messerly, J.F., G.B. Guthrie, S.S. Todd, and H.L. Finke, *Low-temperature thermal data for pentane, n-heptadecane, and n-octadecane. Revised thermodynamic functions for the n-alkanes, C5-C18.* Journal of Chemical & Engineering Data, 1967. **12**(3): p. 338-346.

47. Yokozeki, A., *Solid–liquid phase equilibria of binary indole mixtures with some aromatic compounds using a solid–liquid–vapor equation-of-state.* Applied Energy, 2005. **81**(3): p. 322-333.

48. Carruth, G.F. and R. Kobayashi, *Vapor pressure of normal paraffins ethane through n-decane from their triple points to about 10 mm mercury.* Journal of Chemical & Engineering Data, 1973. **18**(2): p. 115-126.

49. Huber, M.L., A. Laesecke, and R. Perkins, *Transport properties of n-dodecane.* Energy & fuels, 2004. **18**(4): p. 968-975.

Appendix A

Table A-1, Melting and transition temperatures (^{o}K) of the n-paraffins [1].

Number of Carbons in chain	Melting Temperature (T_m) ($\alpha_H - l$)	Melting Temperature (T_m) ($\beta_T - l$)	Transition Temperature (T_m) ($\beta_o - \alpha_H$)	Transition Temperature (T_m)
1		90.67		
2		89.88		
3		85.46		
4		134.8		
5		143.4		
6		177.8		
7		182.5		
8		216.4		
9		219.7	217.2	
10		243.5		
11	247.6		236.6	
12		263.6		
13	267.8		255.0	
14		279		
15	283.1		270.9	
16		291.3		
17	295.1		283.7	
18		301.3		
19	305.2		295.2	
20		309.8		
21	313.4		305.7	
				($\beta_T - \alpha_H$)
22	317.2			316.2
23	320.7		313.7	
24	323.8			321.3
25	326.7		320.2	
				($\beta_M - \alpha_H$)
26	329.5			326.5
27	332.0		326.2	
28	334.4			331.2
29	336.6		331.4	
30	338.6			335.2
31	340.9		335.7	
32	342.5			338.7
33	344.3		340.6*	
				($\beta_M - \beta_o$)
34	345.9		342.6	342.2
35	347.7		345.1	

Cont. of Table A-1, Melting and transition temperatures (^{o}K) of the n-paraffins

Number of Carbons in chain	Melting Temperature (T_m) ($\alpha_H - l$)	Melting Temperature (T_m) ($\beta_T - l$)	Transition Temperature (T_m) ($\beta_o - \alpha_H$)	Transition Temperature (T_m)
36	349.1		347.0	345.3
37	350.6*		348.7*	
38	352.2		350.6*	348.1
39	353.5		352.3*	
40	354.7		353.9*	
41	356.1*		355.5*	
42	357.3*		357.0*	
43	358.5		358.4*	
		($\beta_o - l$)		
44		359.6		
46		361.2		
50		365.3		
52		367.2		
54		368.2		
60		372.4		
62		373.7		
64		375.3		
66		376.8		
67		377.3		
70		378.5		
82		383.5		
94		387.0		
100		388.4		

α_H – Hexagonal, β_o - Orthorhombic, β_T – Triclinic, β_M – Monoclinic
*-

Table A-2, Experimental data of solid-liquid equilibrium measured for some pure hydrocarbons

Compound	P^{s+l}(MPa)	T^{s+l} (K)	ΔH_m (kJmol^{-1})	$P^{\alpha+\beta}$ (MPa)	$T^{\alpha+\beta}$ (K)	ΔH_{tr} (kJmol^{-1})	$\Delta C_{p,m}$(JK^{-1}mol^{-1})	$\Delta C_{p,tr}$(JK^{-1}mol^{-1})	Reference
1-Octanol	24.8 - 183.6	263.2 - 293.2							[37]
	Ambient	258.1	23.7				41.33		[37]
2-methylnaphthalene	19.2 – 265.6	312.3 – 372.6							[6]
Benzene	0.1 – 170.4	278.8 – 323.2							[13]
	Ambient	278.64	9.87						[38]
Cis-1,2-dimethylcyclooctane	202.7 – 242.2	295.7 – 309.1							[6]
Cyclohexane	23.39 – 153.11	293.15 – 353.15							[11]
	0.1 – 74.4	279.7 – 318.2							[13]
	Ambient	280.1/279.65							[11]
	Ambient	279.65	2.677				14.66		[38]
	Ambient	279.8	2.63				14.63		[12]
Cyclooctane	18.4 – 300.8	294.9 – 413.4							[6]
Dotriacontane	Ambient	342.1	76	Ambient	338.9	42.7			[38]
Docosane	Ambient	317.15	39.76	Ambient	315.95	36.35	58.5		[17]
	Ambient	316.8	48.785	Ambient	315.2	29.02			[26]
	Ambient	317.15	49	Ambient	316.25	28.2			[39]
Dodecane	Ambient	263.49	35.86				64.64		[38]
	Ambient	263.46	35.86						[37]
	27.4 - 160.3	268.2 - 293.2							[37]
Eicosane	33.52 – 150	318.15 – 344.91							[10]
	16.27 – 225.04	313.15 – 353.15							[11]
	Ambient	309.85[13]/309.5[7]	66.93[13]/69.73[7]	Ambient	308.65[9]	18.81[13]	54.0[13]		[17]/[11]
	Ambient	311.6	79.16				85.6		[38]
	Ambient	309.5	69.73						[26]
	Ambient	309.75	43.7	Ambient	309.25	26.2			[39]
Heneicosane	Ambient	314.15	47.73	Ambient	306.15	15.49	-100		[17]
	Ambient	313.2	47.697	Ambient	305.6	16.418			[26]
	Ambient	313.35	47.7	Ambient	305.5	15.5			[39]
Heptane	Ambient	182.55	14.04				56.41		[38]
Heptacosane	Ambient	332.65	60.46	Ambient	325.95	28.97	91.5		[17]
	Ambient	331.95	60.3	Ambient	326.25	26.6			[39]
Heptadecane	Ambient	294.9	40.124	Ambient	283.2	10.935			[26]
Hexacosane	Ambient	329.25	59.79	Ambient	326.55	32.82			[39]

Compound	P^{s+l}/MPa	T^{s+l} (K)	ΔH_m (kJmol^{-1})	$P^{\alpha+\beta}$ (MPa)	$T^{\alpha+\beta}$ (K)	ΔH_{tr} (kJmol^{-1})	$\Delta C_{p,m}$(JK^{-1}mol^{-1})	$\Delta C_{p,tr}$(JK^{-1}mol^{-1})	Reference
Hexadecane	9.21 – 309.78	293.15 – 353.15							[11]
	0.1 – 96.5	291.1 – 313.2							[13]
	8.1 - 144.6	293.2 - 323.2							[19]
	Ambient	291.34	53.36				73.55		[38]
	Ambient	329.65[9]/291.2[2]	63.92[9]/53.33[2]	Ambient	326.15[9]	30.36[9]	78.3[9]	77.68[8]	[17]/[11]/[12]
	Ambient	291.2	53.332	Ambient					[26]
Hexatriacontane	Ambient	350.19	91.33	Ambient	348.28	24.72			[38]
	Ambient	349.15		Ambient	347.33	11.73			[38]
Hexane	Ambient	177.8	13.124					44.12	[12]
	Ambient	177.83	13.08	Ambient			46.48		[38]
Hexatriacontane	Ambient	350.19	81.55	Ambient	347.81				[18]
	Ambient	348.95	87.68	Ambient	347				[18]
	Ambient	348.8	91.33	Ambient	345.2				[18]
	Ambient	349.15	88.74	Ambient	346.1				[18]
	Ambient	349.05	88.83	Ambient	346.11				[18]
	Ambient	348.94	87.68						[18]
Methane	Ambient	90.7	0.94						[26]
Naphthalene	Ambient	354.69	19.55						[38]
	Ambient	353.4	18.24						[38]
Nonadecane	Ambient	305.05	45.38	Ambient	296.95	13.81	-332.8		[17]
	Ambient	304.9	45.58	Ambient	295.5	13.75			[26]
	Ambient	305.15	43.75	Ambient	295.75	13.75			[39]
Octacosane	Ambient	334.65	66.52	Ambient	331.35	33.66	118.9		[17]
	Ambient	333.9	66.52	Ambient	331.15	33.6	118.9		[38]
	Ambient	334.35	64.7	Ambient	331.25	35.5			[39]
Octadecane	11.29 – 309.78	303.15 – 353.15							[11]
	Ambient	301.45	61.71					71.2	[38]
	Ambient	301.95[13]/301.2[7]	61.71[13]/61.306[7]				50[13]	80.84[8]	[17]/[11]/[12]
	Ambient	301.2	61.306						[26]
	Ambient	301.32	61.71	Ambient	299.95				[39]
Octane	Ambient	216.32	20.74				53.85		[38]
	Ambient	216.52	20.74						[37]
	0.1 - 300	216.2 - 269.2							[37]
o-Xylene	210.2 – 262.5	295.0 – 307.1							[6]
p-Xylene	26.9 – 261.4	295.1 – 367.1							[6]

Compound	P^{s+l}/MPa	T^{s+l} (K)	ΔH_m (kJmol^{-1})	$P^{\alpha+\beta}$ (MPa)	$T^{\alpha+\beta}$ (K)	ΔH_{tr} (kJmol^{-1})	$\Delta C_{p,m}$(JK^{-1}mol^{-1})	$\Delta C_{p,tr}$(JK^{-1}mol^{-1})	Reference
Pentacosane	Ambient	325.92	55.53	Ambient	310.95	23.9			[18]
	Ambient	326.3	57.09	Ambient	320.3	26.67			[18]
	Ambient	326	54.04	Ambient	319.3	24.43			[18]
	Ambient	326.9	57.78	Ambient	320.08	26.08			[18]
	Ambient	325.9	57.78	Ambient	312.9	1.07	71		[38]
				Ambient	309	23.9			[38]
		326.65	56.58		318.74				[18]
	Ambient	326.65	57.8	Ambient	320.1	26.1			[39]
Pentacontane	Ambient	364.75	163.468						[38]
Pentadecane	Ambient	283.1	34.574	Ambient	270.9	9.162			[26]
Propane	Ambient	85.5	3.527						[26]
Tetracosane	Ambient	324.05	57.31	Ambient	320.55	27.68	66.6		[17]
	Ambient	323.75	54.93	Ambient	321.25	31.3	66.6		[38]
	Ambient	323.5	54	Ambient	321.45	31.5			[39]
Tetracontane	10 – 130	357.34 – 385.22		10 – 50	324.24 – 334.94				[10]
	10 – 130	357.34 – 385.22		10 – 73.917	351.37 – 371.15				[10]
Tetradecane	0.1 – 183.1	278.6 – 318.2							[13]
	16.0 - 183.1	283.2 - 318.2							[19]
	Ambient	279.03	45.07				71.17		[38]
	279	45.03							[26]
Tricosane	Ambient	321.65	54.01	Ambient	315.35	21.77	0.1		[17]
	Ambient	323.6	54.396	Ambient	320.7	31.701			[26]
	Ambient	320.65	54	Ambient	313.85	21.8			[39]
Trans-1,4-dimethylcyclohexane	172.1 – 273.3	295.2 – 326.3							[6]
Triacontane	10 – 150	341.68 – 372.97		10 – 75	338.9 – 356.07				[10]
	Ambient	338.11	67.07	Ambient	335.25	37.49			[38]
Tridecane	134.32 – 582.04	293.15 – 353.15							[11]
	Ambient	267.6	28.485	Ambient	255	9.162		-105.94	[11]
	Ambient	267.6	28.485	Ambient	255	7.656			[26]
Undecane	Ambient	247.54	22.3				-49.2		[38]

T^{s+l} and P^{s+l} are the melting temperature and pressure, $T^{\alpha+\beta}$ and $P^{\alpha+\beta}$ are the temperature and pressure of the transition solid α – solid β; molar enthalpy of fusion ΔH_m; molar heat of transition (α – β) ΔH_{tr}; heat capacity change at the melting temperature $\Delta C_{p,m}$; heat capacity change at the transition temperature $\Delta C_{p,tr}$

Table A-3, Experimental data of solid-liquid equilibrium for binary hydrocarbon mixture

Components	Mole fraction x_1	P (MPa)	T (K)	Reference
1-Octanol (1) + n-hexadecane (2)	0.200 - 0.972	5.3 - 230.9	275.2 - 332.6	[19]
1-Octanol (1) + n-tetradecane (2)	0.239 - 0.948	16.1 - 178.5	263.2 - 313.2	[19]
Tridecane (1) + cyclohexane (2)	0.0 - 1.0	23.39 – 582.04	293.15 – 353.15	[11]
Hexadecane (1) + cyclohexane (2)	0.0 - 1.0	9.21 – 678.27	293.15 – 353.15	[11]
Octadecane (1) + cyclohexane (2)	0.0 - 1.0	11.29 – 455.10	303.15 – 353.15	[11]
Eicosane (1) + cyclohexane (2)	0.0 - 1.0	16.27 – 499.38	313.15 – 363.15	[11]
Benzene (1) + n-Tetradecane (2)	0.0 - 1.0	0.1 – 224.9	264.90 – 323.2	[13]
Benzene (1) + n-Hexadecane (2)	0.0 - 1.0	0.1 – 188.5	272.20 – 323.2	[13]
Cyclohexane (1) + n-Tetradecane (2)	0.19 – 0.95	0.1 – 146.8	251.10 – 318.2	[13]
Cyclohexane (1) + n-Hexadecane (2)	0.20 – 0.96	0.1 – 124.5	261.7 – 313.2	[13]
n-Triacontane (1) + methane (2)	0.02 – 1.0	18.10 – 193.10	335.25 – 382.29	[15]
n-Hexadecane (1) + n-Tetradecane (2)	0.0 – 1.0	0.1 – 100	276.2 – 313.5	[4]
n-Pentadecane (1) + n-Tetradecane (2)	0.0 – 1.0	0.1 – 100	276.1 – 303.9	[4]
n-Tridecane (1) + n-Hexane (2)	0.0232 – 1.0	133.01 – 1163.74	293.15 – 343.15	[12]
n-Eicosane (1) + methane (2)	0.0492 - 1.0	1.36 - 98.10	303.75 - 331.19	[40]
n-Hexadecane (1) + n-Hexane (2)	0.0260 – 1.0	9.21 – 1045.01	293.15 – 343.15	[12]
n-Octadecane (1) + n-Hexane (2)	0.0608 – 1.0	8.86 – 677.49	293.15 – 343.15	[12]
n-Eicosane (1) + Ethylene (2)	0.089 - 0.221	6.16 - 50.23	302.50 - 291.91	[20]
n-Tetracontane (1) + Propane (2)	0.005 - 0.039	2.63 - 95.35	322.68 - 344.23	[20]
Methane (1) + Tetracosane (2)	0.003 - 1.0	0.10 - 257.50	313.93 - 375.98	[16]
1-Octanol (1) + n-Octane (2)	0.1 - 0.8	47.1 - 201.0	101.2 - 292.9	[37]
1-Octanol (1) + n-Dodecane (2)	0.25 - 0.945	20.1 - 174.7	263.2 - 293.2	[37]

Table A-4, Values of eutectic pressures, temperatures and compositions for binary mixtures

Components	Mole fraction x_e	P_e (MPa)	T_e (K)	Reference
Tridecane (1) + cyclohexane (2)	0.144 – 0.199	0.1 – 300	239.1 – 291.6	[11]
Hexadecane (1) + cyclohexane (2)	0.074 – 0.143	0.1 – 300	256.2 – 314.2	[11]
Octadecane (1) + cyclohexane (2)	0.051 – 0.135	0.1 – 300	266.8 – 326.8	[11]
Eicosane (1) + cyclohexane (2)	0.035 – 0.108	0.1 – 250	271.2 – 326.2	[11]
1-Octanol (1) + n-Octane (2)	0.0023	Ambient	216.3	[37]
1-Octanol (1) + n-Dodecane (2)	0.826	Ambient	254.61	[37]

Table A-5, Specific Heat Capacity of solids and liquids for some hydrocarbons

Compounds	Pressure Range (MPa)	Temperature Range (K)	Cp^S cal/g	Cp^L cal/g	Reference
2-methylbutane	Ambient	80.4 - 215.8	0.217 - 0.279	0.409 - 0.521	[41]
n-Hexane	Ambient	89.7 - 295.1	0.218 - 0.331	0.468 - 0.531	[41]
n-Heptane	Ambient	90.1 - 262.5	0.205 - 0.295	0.48 - 0.53	[41]
2-Methylhexane	Ambient	85.9 - 225	0.202 - 0.306	0.427 - 0.523	[41]
n-Octane	Ambient	85.5 - 293.7	0.188 - 0.372	0.482 - 0.518	[41]
2,2,4-Trimethylpentane	Ambient	87.9 - 295.2	0.181 - 0.325	0.388 - 0.489	[41]
Hexamethylethane	Ambient	88.8 - 295.4	0.166 - 0.486		[41]
n-Nonane	Ambient	224.5 - 299.1		0.484 - 0.524	[41]
n-Decane	Ambient	242.3 - 295.5		0.483 - 0.520	[41]
Di-iso-Amyl	Ambient	223.2 - 295		0.453 - 0.507	[41]
n-Eicosane	Ambient	93.6 - 279.1	0.175 - 0.512		[41]
n-Tritriacontane	Ambient	93.7 - 294.4	0.168 - 0.463		[41]
Cyclohexane	Ambient	91.8 - 298.9	0.157 - 0.362	0.422 - 0.440	[41]
Propylene	Ambient	68.9 - 210.3	0.273 - 0.317	0.523 - 0.512	[42]
n-Butane	Ambient	69.1 - 261.8	0.212 - 119.9	0.467 - 0.533	[42]
n-Hexane	Ambient	93.4 - 293.5	0.219 - 0.328	0.472 - 0.536	[42]
n-Octane	Ambient	92.4 - 298.3	0.198 - 0.346	0.483 - 0.526	[42]
n-Nonane	Ambient	92.8 - 297.9	0.195 - 0.322	0.489 - 0.523	[42]
n-Decane	Ambient	91.3 - 220.6	0.188 - 0.355	0.495 - 0.523	[42]
n-Undecane	Ambient	92 - 298	0.188 - 0.338	0.503 - 0.524	[42]
n-Dodecane	Ambient	93.3 - 297.7	0.184 - 0.380	0.510 - 0.521	[42]
Methylcyclopentane	Ambient	92.2 - 293.7	0.183 - 0.230	0.352 - 0.447	[42]
1,2-Dimethylcyclopentane	Ambient	93.4 - 294.2	0.191 - 0.263	0.364 - 0.456	[42]
Pseudocumene	Ambient	93.7 - 297.3	0.158 - 0.307	0.388 - 0.422	[42]
Durene	Ambient	92.2 - 297.1	0.156 - 0.383		[42]
Isodurene	Ambient	92.4 - 297.1	0.162 - 0.302	0.401 - 0.428	[42]
Prehnitene	Ambient	91 - 291.9	0.149 - 0.328	0.416 - 0.420	[42]
p-Cymene	Ambient	92.2 - 297.1	0.156 - 0.269	0.367 - 0.421	[42]
n-Butylbenzene	Ambient	94.0 - 298.2	0.154 - 0.231	0.369 - 0.428	[42]
Pentamethylbenzene	Ambient	91.7 - 303.6	0.169 - 0.447		[42]
β-Methylnaphthalene	Ambient	93.8 - 310.4	0.121 - 0.299	0.383	[42]
Anthracene	Ambient	94.4 - 297.2	0.095 - 0.278		[42]
Phenanthrene	Ambient	93.4 - 304.4	0.097 - 0.325		[42]

Table A-6, Specific Heat Capacity of solids and liquids for some hydrocarbons

Compounds	Pressure Range (MPa)	Temperature Range (K)	Cp^S $Jg^{-1}K^{-1}$	Cp^L $Jg^{-1}K^{-1}$	Reference
Cyclohexane	0.1	293.15 - 333.15		1.824 - 1.997	[43]
Toluene	0.1 - 20	273.15 - 333.15		1.593 - 1.825	[43]
Dimethylethyl ether	0.1 - 21	273.15 - 333.16		1.974 - 2.308	[43]

Table A-7, Specific Heat Capacity of solids and liquids for some hydrocarbons

Compounds	Pressure Range (MPa)	Temperature Range (K)	Cp^S $calmol^{-1}K^{-1}$	Cp^L $calmol^{-1}K^{-1}$	Reference
n-Octane	Ambient	12.60 - 297.58	0.885 - 41.237	55.590 - 60.680	[44]
n-Nonane	Ambient	11.93 - 313.88	0.837 - 233	63.264 - 69.699	[44]
n-Decane	Ambient	12.28 - 318.62	0.873 - 60.440	70.973 - 77.588	[44]
n-Undecane	Ambient	12.15 - 298.92	0.967 - 86.517	78.838 - 82.515	[44]
n-Dodecane	Ambient	11.82 - 317.41	0.850 - 92.282		[44]
n-Tridecane	Ambient	11.78 - 306.38	0.950 - 114.6	94.950 - 98.298	[44]
n-Tetradecane	Ambient	12.09 - 302.77	1.004 - 81.923	103.186 - 105.352	[44]
n-Pentadecane	Ambient	11.84 - 312.78	1.031 - 150.7	111.161 - 114.233	[44]
n-Hexadecane	Ambient	11.90 - 320.28	1.052 - 95.164	119.622 - 123.091	[44]

Table A-8, Extracted Solid-Liquid Equilibrium Data for Pure Hydrocarbons

Cyclohexane		n-Eicosane		n-Octadecane		n-Hexadecane		Tridecane	
P_{tp} (kPa)[45]	5.388	P_{tp} (MPa)		P_{tp} (MPa)		P_{tp} (MPa)		P_{tp} (MPa)	
T_{tp} (K)[45]	279.48	T_{tp} (K) [39]	309.64	T_{tp} (K)[46]	301.3	T_{tp} (K)		T_{tp} (K)	
ΔH_m (kJmol^{-1})[12]	2.63	ΔH_m (kJmol^{-1})[11]	69.73	ΔH_m (kJmol^{-1})[17]	61.71	ΔH_m (kJmol^{-1})[3]	53.33	ΔH_m (kJmol^{-1})[26]	28.485
P^{s+l}(MPa)[13]	T^{s+l} (K)[13]	P^{s+l}(MPa)[11]	T^{s+l} (K)[11]	P^{s+l}(MPa)[11]	T^{s+l} (K)[11]	P^{s+l}(MPa)[11]	T^{s+l} (K)[11]	P^{s+l}(MPa)[11]	T^{s+l} (K)[11]
0.1	279.7	16.27	313.15	11.29	303.15	9.21	293.15	134.32	293.15
9.2	283.2	44.59	323.15	50.28	313.15	50.65	303.15	197.41	303.15
17.7	288.2	88.83	333.15	94.64	323.15	95.56	313.15	265.12	313.15
26	293.2	148.97	343.15	144.37	333.15	143.92	323.15	337.43	323.15
36.3	298.2	225.04	353.15	199.48	343.15	195.74	333.15	414.35	333.15
46.5	303.2			259.95	353.15	251.03	343.15	495.89	343.15
53.9	308.2					309.78	353.15	582.04	353.15
60.8	313.2								
74.4	318.2								

n-Triacontane	
P_{tp} (MPa)	
T_{tp} (K)	
ΔH_m (kJmol^{-1})[38]	67.07
P^{s+l}(MPa)[10]	T^{s+l} (K)[10]
10	341.68
25	345.34
50	351.45
75	357
100	362.54
125	367.76
150	372.97

n-Triacontane	
ΔH_{tr} (kJmol^{-1})[38]	37.49
$P^{\alpha+\beta}$ (MPa)[10]	$T^{\alpha+\beta}$ (K)[10]
10	338.9
25	343.03
50	349.8
75	356.07

n-Tetracosane	
P_{tp} (MPa)	
T_{tp} (K)	
ΔH_m (kJmol^{-1})[38]	54.93
P^{s+l}(MPa)[10]	T^{s+l} (K)[10]
10	326.74
25	330.4
40	333.86
50	336.12
100	346.93
125	352.26
150	357.28

n-Tetracosane	
ΔH_{tr} (kJmol^{-1})[38]	31.3
$P^{\alpha+\beta}$ (MPa)[10]	$T^{\alpha+\beta}$ (K)[10]
10	338.9
25	343.03
50	349.8
75	356.07

n-Tetracontane	
ΔH_{tr} (kJmol^{-1})	
$P^{\alpha+\beta}$ (MPa)[10]	$T^{\alpha+\beta}$ (K)[10]
10	351.37
48.436	363.15
50	363.15
73.917	364.54

n-Tetracontane	
P_{tp} (MPa)	
T_{tp} (K)	
ΔH_m (kJmol^{-1})	
P^{s+l}(MPa)[11]	T^{s+l} (K)[11]
10	357.34
35.758	363.15
50	367.26
68.114	371.15
90	376.58
112.74	381.15
130	385.22

trans-1,4-DimethylcycloC6		Cyclooctane		cis-1,2-DimethylcycloC6		n-Tetradecane		o-Xylene	
P_{tp} (MPa)		P_{tp} (MPa)		P_{tp} (MPa)		P_{tp} (MPa)		P_{tp} (MPa)	
T_{tp} (K)		T_{tp} (K)		T_{tp} (K)		T_{tp} (K)		T_{tp} (K)	
ΔH_m (kJmol^{-1})		ΔH_m (kJmol^{-1})		ΔH_m (kJmol^{-1})		ΔH_m (kJmol^{-1})[38]	45.07	ΔH_m (kJmol^{-1})	
P^{s+l}(MPa)[6]	T^{s+l} (K)[6]	P^{s+l}(MPa)[6]	T^{s+l} (K)[6]	P^{s+l}(MPa)[3]	T^{s+l} (K)[4]	P^{s+l}(MPa)[13]	T^{s+l} (K)[13]	P^{s+l}(MPa)[6]	T^{s+l} (K)[6]
172.1	295.2	18.4	294.9	202.7	295.7	0.1	278.6	210.2	295
181.3	298.3	63.4	314.9	212.4	298.6	16	283.2	211.6	295.4
193.5	302.1	103.7	333.5	217.2	300.5	37.3	288.2	212.4	295.6
199.3	303.9	143.5	351.4	219.9	301.5	58.2	293.2	220.6	297.4
216	309.1	196.2	373.8	230.2	304.8	80.9	298.2	223.4	298.1
227.9	312.6	247.6	394.4	242.2	309.1	107.5	303.2	223.7	298.2
236.7	315.6	300.8	413.4			133.1	308.2	223.8	298.3
252.3	320.3					163.5	313.2	228.4	299.4
266.7	324.5					183.1	318.2	238.4	301.9
273.3	326.3							243.7	303.1
								251	304.7
								262.5	307.1

n-Dodecane	
P_{tp} (kPa)	
T_{tp} (K) [49]	263.59
ΔH_m (kJmol^{-1})[37]	35.86
P^{s+l}(MPa)[37]	T^{s+l} (K)[37]
27.4	268.2
50	273.2
74.5	278.2
104	283.2
132.3	288.2
160.3	293.2

Benzene		2-Methylnaphthalene		p-Xylene		1-Octanol		n-Octane	
P_{tp} (kPa)[47]	4.979	P_{tp} (kPa)[47]	0.073	P_{tp} (MPa)					
T_{tp} (K)[47]	278.7	T_{tp} (K)[47]	307.72	T_{tp} (K)		P_{tp} (MPa)		P_{tp} (kPa)[48]	0.0021998
ΔH_m (kJmol^{-1})[38]	9.87	ΔH_m (kJmol^{-1})		ΔH_m (kJmol^{-1})		T_{tp} (K)		T_{tp} (K)[48]	216.37
P^{s+l}(MPa)[13]	T^{s+l} (K)[13]	P^{s+l}(MPa)[11]	T^{s+l} (K)[11]	P^{s+l}(MPa)[6]	T^{s+l} (K)[6]	ΔH_m (kJmol^{-1})[37]	23.7	ΔH_m (kJmol^{-1})[37]	20.74
278.8	0.1	30.1	314.8	26.9	295.1	P^{s+l}(MPa)[37]	T^{s+l} (K)[37]	P^{s+l}(MPa)[37]	T^{s+l} (K)[37]
283.2	12.6	52.3	320.3	53.3	304	24.8	263.2	0.1	216.2
288.2	31.6	77.2	326.4	87.8	315.2	50.3	268.2	50	226.7
293.2	51.6	124.1	339.1	120.3	325.6	76.2	273.2	100	236.2
298.2	69.5	153.9	346.4	150.5	335	102.3	278.2	150	245.2
303.2	88.1	188.1	355	185.5	345.6	129.2	283.2	200	254.2
308.2	108.2	209.2	359.6	213.1	353.8	156.3	288.2	250	262.2
313.2	123.8	227.8	364.2	226.8	357.7	183.6	293.2	300	269.2
318.2	150.8	245.1	368.1	246.3	363.2				
323.2	170.4	265.6	372.6	261.4	367.1				

Appendix B

Table B-1, Freezing Temperature profile for pure Dodecane

Pure Dodecane-Freezing									
Time(min)	SampleTp.°C	Time(min)	SampleTp.°C	Time(min)	SampleTp.°C	Time(min)	SampleTp.°C	Time(min)	SampleTp. °C
0	24.5	72	-1.7	144	-9.6	216	-9.7	288	-11.6
2	24.5	74	-2.1	146	-9.6	218	-9.7	290	-11.9
4	24.4	76	-2.7	148	-9.6	220	-9.7	292	-12.2
6	24	78	-3.1	150	-9.6	222	-9.7	294	-12.5
8	23.6	80	-3.6	152	-9.6	224	-9.7	296	-12.9
10	23.1	82	-3.9	154	-9.6	226	-9.7	298	-13.3
12	22.5	84	-4.3	156	-9.6	228	-9.7	300	-13.7
14	21.9	86	-4.7	158	-9.6	230	-9.7	302	-14.2
16	21.2	88	-5	160	-9.6	232	-9.7	304	-14.6
18	20.4	90	-5.3	162	-9.6	234	-9.8	306	-15.1
20	19.7	92	-5.6	164	-9.6	236	-9.8	308	-15.7
22	19	94	-5.9	166	-9.6	238	-9.8	310	-16.2
24	18.3	96	-6.1	168	-9.6	240	-9.8	312	-16.9
26	17.5	98	-6.5	170	-9.6	242	-9.8	314	-17.5
28	16.6	100	-6.7	172	-9.6	244	-9.8	316	-18.3
30	15.8	102	-6.9	174	-9.6	246	-9.8	318	-19.1
32	14.9	104	-7.2	176	-9.6	248	-9.8	320	-19.9
34	14	106	-7.5	178	-9.6	250	-9.8	322	-20.8
36	13.3	108	-7.7	180	-9.6	252	-9.8	324	-21.7
38	12.3	110	-7.9	182	-9.6	254	-9.9	326	-22.6
40	11.4	112	-8.1	184	-9.6	256	-9.9	328	-23.5
42	10.6	114	-8.3	186	-9.6	258	-9.9	330	-24.3
44	9.7	116	-8.5	188	-9.6	260	-10	332	-25.1
46	8.8	118	-8.7	190	-9.7	262	-10	334	-25.5
48	7.9	120	-8.9	192	-9.7	264	-10.1	336	-26
50	7.1	122	-9.2	194	-9.7	266	-10.1	338	-26.3
52	6.1	124	-9.4	196	-9.7	268	-10.2		
54	5.2	126	-9.6	198	-9.7	270	-10.3		
56	4.3	128	-9.7	200	-9.7	272	-10.4		
58	3.4	130	-9.9	202	-9.7	274	-10.5		
60	2.4	132	-10.1	204	-9.7	276	-10.6		
62	1.7	134	-9.6	206	-9.7	278	-10.7		
64	0.9	136	-9.6	208	-9.7	280	-10.8		
66	0.2	138	-9.6	210	-9.7	282	-11		
68	-0.5	140	-9.6	212	-9.7	284	-11.2		
70	-1.1	142	-9.6	214	-9.7	286	-11.4		

Table B-2, Melting Temperature profile for pure Dodecane

Pure Dodecane									
Melting									
Time(min)	Sample Tp.°C	Time(min)	Sample Tp.°C	Time(min)	Sample Tp.°C	Time(min)	Sample Tp.°C	Time(min)	Sample Tp.°C
0	-38.2	72	-26.4	144	-19.3	216	-12.8	288	-10.1
2	-38.2	74	-26.2	146	-19.1	218	-12.7	290	-10.1
4	-38.2	76	-26	148	-18.9	220	-12.5	292	-10.1
6	-38.2	78	-25.8	150	-18.7	222	-12.3	294	-10
8	-38.1	80	-25.5	152	-18.6	224	-12.2	296	-10
10	-38	82	-25.3	154	-18.4	226	-12.1	298	-9.9
12	-37.8	84	-25.1	156	-18.2	228	-11.9	300	-9.9
14	-37.4	86	-24.9	158	-18.1	230	-11.7	302	-9.9
16	-37	88	-24.7	160	-17.9	232	-11.6	304	-9.8
18	-36.5	90	-24.6	162	-17.7	234	-11.6	306	-9.7
20	-36	92	-24.4	164	-17.5	236	-11.4	308	-9.7
22	-35.4	94	-24.2	166	-17.3	238	-11.3	310	-9.7
24	-34.9	96	-24	168	-17.1	240	-11.2	312	-9.7
26	-34.4	98	-23.8	170	-16.9	242	-11.2	314	-9.6
28	-33.8	100	-23.6	172	-16.7	244	-11.1	316	-9.6
30	-33.1	102	-23.4	174	-16.5	246	-11	318	-9.6
32	-32.6	104	-23.2	176	-16.3	248	-10.9	320	-9.6
34	-32	106	-23	178	-16.2	250	-10.8	322	-9.6
36	-31.7	108	-22.8	180	-16	252	-10.7	324	-9.6
38	-31.2	110	-22.6	182	-15.8	254	-10.7	326	-9.6
40	-30.8	112	-22.4	184	-15.6	256	-10.6	328	-9.6
42	-30.4	114	-22.2	186	-15.4	258	-10.5	330	-9.6
44	-30	116	-22	188	-15.3	260	-10.5	332	-9.6
46	-29.7	118	-21.8	190	-15.1	262	-10.4	334	-9.6
48	-29.4	120	-21.7	192	-14.9	264	-10.4	336	-9.6
50	-29	122	-21.4	194	-14.7	266	-10.4	338	-9.6
52	-28.9	124	-21.3	196	-14.5	268	-10.3	340	-9.6
54	-28.5	126	-21.1	198	-14.3	270	-10.3	342	-9.6
56	-28.2	128	-20.9	200	-14.1	272	-10.3	344	-9.6
58	-27.9	130	-20.7	202	-14	274	-10.2	346	-9.5
60	-27.8	132	-20.5	204	-13.8	276	-10.2	348	-9.5
62	-27.4	134	-20.3	206	-13.6	278	-10.2	350	-9.5
64	-27.2	136	-20.1	208	-13.5	280	-10.2	352	-9.4
66	-27	138	-19.9	210	-13.4	282	-10.2	354	-9.4
68	-26.8	140	-19.7	212	-13.2	284	-10.1	356	-9.3
70	-26.6	142	-19.5	214	-13	286	-10.1	358	-9.2

Pure Dodecane			
Melting			
Time(min)	Sample Tp.°C	Time(min)	Sample Tp.°C
360	-9	434	7.3
362	-8.8	436	7.9
364	-8.6	438	8.7
366	-8.3	440	9.2
368	-8.1	442	10.2
370	-7.4	444	11.1
372	-7.4	446	12.3
374	-6.7	448	13.7
376	-5.8	450	15.1
378	-5.1	452	16.7
380	-4.4	454	17.8
382	-3.7	456	18.9
384	-3.2	458	19.8
386	-2.6	460	20.6
388	-2	462	21.3
390	-1.6	464	21.9
392	-1.2	466	22.3
394	-1	468	22.9
396	-0.7	470	23
398	-0.4		
400	-0.1		
402	0.1		
404	0.4		
406	0.7		
408	1.1		
410	1.3		
412	1.6		
414	1.9		
416	2.2		
418	2.5		
420	3.1		
422	3.5		
424	3.9		
426	4.5		
428	5.1		
430	5.8		
432	6.5		

Table B-3, Freezing temperature profile for mixture of Decane and Dodecane

$0.1518C_{10} + 0.8482C_{12}$											
Freezing											
Time(min)	Sample Tp.ºC	Time(min)	Sample Tp.ºC	Time(min)	Sample Tp.ºC	Time(min)	Sample Tp.ºC	Time(min)	Sample Tp.ºC	Time(min)	Sample Tp.ºC
0	20.5	62	-2	124	-10.5	186	-12.4	248	-13.8	310	-20.4
2	20.7	64	-2.4	126	-10.7	188	-12.4	250	-14	312	-20.6
4	20.4	66	-2.9	128	-10.9	190	-12.5	252	-14.3		
6	19.9	68	-3.3	130	-11.2	192	-12.5	254	-14.5		
8	19.3	70	-3.7	132	-11.4	194	-12.4	256	-14.7		
10	18.8	72	-4.1	134	-11.6	196	-12.5	258	-15		
12	18	74	-4.5	136	-11.8	198	-12.6	260	-15.2		
14	17.4	76	-5	138	-11.9	200	-12.5	262	-15.3		
16	16.6	78	-5.1	140	-12	202	-12.5	264	-15.5		
18	15.9	80	-5.5	142	-12.2	204	-12.5	266	-15.7		
20	15.1	82	-5.7	144	-12.4	206	-12.5	268	-15.9		
22	14.4	84	-6.1	146	-12.6	208	-12.6	270	-16.2		
24	13.4	86	-6.3	148	-12.8	210	-12.5	272	-16.4		
26	12.6	88	-6.6	150	-13	212	-12.6	274	-16.6		
28	11.8	90	-6.9	152	-12.7	214	-12.6	276	-16.9		
30	11	92	-7.1	154	-12.2	216	-12.7	278	-17.1		
32	10.1	94	-7.4	156	-12.2	218	-12.6	280	-17.4		
34	9.2	96	-7.6	158	-12.2	220	-12.7	282	-17.6		
36	8.4	98	-7.8	160	-12.2	222	-12.7	284	-17.7		
38	7.4	100	-8.1	162	-12.2	224	-12.7	286	-17.9		
40	6.6	102	-8.3	164	-12.2	226	-12.7	288	-18.1		
42	5.7	104	-8.5	166	-12.2	228	-12.8	290	-18.3		
44	4.8	106	-8.7	168	-12.3	230	-12.8	292	-18.5		
46	3.9	108	-8.9	170	-12.3	232	-12.8	294	-18.7		
48	3	110	-9.1	172	-12.3	234	-12.8	296	-18.9		
50	2.1	112	-9.3	174	-12.3	236	-12.9	298	-19.1		
52	1.2	114	-9.6	176	-12.3	238	-12.9	300	-19.3		
54	0.5	116	-9.7	178	-12.4	240	-13	302	-19.5		
56	-0.2	118	-10	180	-12.4	242	-13.2	304	-19.8		
58	-0.9	120	-10.2	182	-12.4	244	-13.5	306	-20		
60	-1.5	122	-10.4	184	-12.4	246	-13.6	308	-20.2		

Table B-4, Freezing and melting temperature profile for mixture of Decane and Dodecane

$0.2470C_{10} + 0.75306C_{12}$									
Freezing						Melting			
Time(min)	Sample Tp°C	Time(min)	Sample Tp°C	Time(min)	Sample Tp°C	Time(min)	Sample Tp.°C	Time(min)	Sample Tp.°C
0	-8.7	62	-14	124	-15	0	-20.5	62	-15
2	-8.9	64	-14	126	-15.1	2	-20.2	64	-14.7
4	-9.3	66	-14.1	128	-15.1	4	-20	66	-14.4
6	-9.7	68	-14.1	130	-15.2	6	-19.9	68	-14
8	-10	70	-14.1	132	-15.3	8	-19.6	70	-13.5
10	-10.3	72	-14.1	134	-15.4	10	-19.4	72	-12.9
12	-10.6	74	-14.1	136	-15.5	12	-19.2	74	-12.3
14	-10.9	76	-14.1	138	-15.5	14	-19.1	76	-11.6
16	-11.1	78	-14.2	140	-15.6	16	-18.9	78	-10.6
18	-11.4	80	-14.2	142	-15.7	18	-18.7	80	-9.5
20	-11.6	82	-14.2	144	-15.9	20	-18.6	82	-8.9
22	-11.8	84	-14.2	146	-16	22	-18.4	84	-8.2
24	-12.1	86	-14.2	148	-16.2	24	-18.3	86	-7.4
26	-12.4	88	-14.2	150	-16.3	26	-18.1	88	-6.8
28	-12.5	90	-14.2	152	-16.5	28	-17.9	90	-6.1
30	-12.8	92	-14.3	154	-16.7	30	-17.7	92	-5.4
32	-13	94	-14.3	156	-16.9	32	-17.5	94	-4.5
34	-13.2	96	-14.4	158	-17.1	34	-17.3		
36	-13.5	98	-14.4	160	-17.3	36	-17.2		
38	-13.7	100	-14.5	162	-17.5	38	-17		
40	-14	102	-14.5	164	-17.7	40	-16.8		
42	-14.1	104	-14.6	166	-17.9	42	-16.6		
44	-14.3	106	-14.6	168	-18.2	44	-16.5		
46	-14.5	108	-14.6	170	-18.4	46	-16.4		
48	-14.7	110	-14.7	172	-18.6	48	-16.3		
50	-15.9	112	-14.7	174	-18.8	50	-16.1		
52	-15	114	-14.7	176	-19.2	52	-16		
54	-14.3	116	-14.8	178	-19.3	54	-15.8		
56	-14.1	118	-14.8	180	-19.8	56	-15.6		
58	-14	120	-14.9	182	-20	58	-15.4		
60	-14	122	-14.9			60	-15.2		

Table B-5, Freezing temperature profile for mixture of Decane and Dodecane

$0.5386C_{10} + 0.0.4614C_{12}$									
Freezing									
Time(min)	Sample Tp.^{o}C	Time(min)	Sample Tp.^{o}C	Time(min)	Sample Tp.^{o}C	Time(min)	Sample Tp.^{o}C	Time(min)	Sample Tp.^{o}C
0	-5.5	62	-9.9	124	-21.9	186	-24.2	248	-28.7
2	-5.6	64	-10	126	-22.4	188	-24.4	250	-28.8
4	-5.7	66	-10.1	128	-22.7	190	-24.3	252	-29
6	-5.7	68	-10.3	130	-23.1	192	-24.4	254	-29.3
8	-5.8	70	-10.5	132	-23.5	194	-24.5	256	-29.6
10	-5.9	72	-10.7	134	-23.6	196	-24.6	258	-29.9
12	-6	74	-10.9	136	-24	198	-24.7	260	-30
14	-6.1	76	-11.1	138	-24.4	200	-24.8	262	-30.3
16	-6.2	78	-11.3	140	-24.5	202	-24.9	264	-30.5
18	-6.3	80	-11.4	142	-24.6	204	-25.1	266	-30.7
20	-6.4	82	-11.7	144	-24.8	206	-25.2	268	-30.9
22	-6.6	84	-11.8	146	-24.9	208	-25.2	270	-31.2
24	-6.7	86	-12	148	-24.8	210	-25.4	272	-31.3
26	-6.9	88	-12.3	150	-25	212	-25.6	274	-31.5
28	-7.1	90	-12.4	152	-25.1	214	-25.7	276	-31.7
30	-7.3	92	-12.6	154	-25.2	216	-25.9	278	-32
32	-7.4	94	-12.8	156	-25.1	218	-26.1	280	-32.3
34	-7.6	96	-13	158	-25.1	220	-26.2	282	-32.4
36	-7.7	98	-13.1	160	-25.1	222	-26.4	284	-32.7
38	-7.9	100	-13.7	162	-25.1	224	-26.5	286	-32.8
40	-8.1	102	-14.2	164	-25.1	226	-26.7	288	-33.1
42	-8.2	104	-15	166	-25	228	-26.8	290	-33.3
44	-8.4	106	-16.4	168	-24.8	230	-26.9	292	-33.5
46	-8.5	108	-17	170	-24.6	232	-27.2	294	-33.7
48	-8.6	110	-17.7	172	-24.4	234	-27.3		
50	-8.7	112	-17.9	174	-24.2	236	-27.5		
52	-8.9	114	-18	176	-24.2	238	-27.7		
54	-9.2	116	-20	178	-24.1	240	-27.9		
56	-9.3	118	-20.4	180	-24	242	-28.1		
58	-9.5	120	-20.8	182	-24.1	244	-28.3		
60	-9.7	122	-21.3	184	-24.1	246	-28.4		

Table B-6, Melting temperature profile for mixture of Decane and Dodecane

$0.5386C_{10} + 0.0.4614C_{12}$									
Melting									
Time(min)	Sample Tp.^{o}C	Time(min)	Sample Tp.^{o}C	Time(min)	Sample Tp.^{o}C	Time(min)	Sample Tp.^{o}C	Time(min)	Sample Tp.^{o}C
0	-34	62	-29.2	124	-25.2	186	-21.2	248	-11.3
2	-33.9	64	-29	126	-25.1	188	-21	250	-10.7
4	-33.9	66	-28.8	128	-25.1	190	-20.8	252	-10.4
6	-33.8	68	-28.6	130	-25	192	-20.5	254	-9.7
8	-33.7	70	-28.5	132	-25	194	-20.3	256	-9.2
10	-33.7	72	-28.3	134	-24.9	196	-19.9	258	-8.5
12	-33.7	74	-28.1	136	-24.9	198	-19.5	260	-7.3
14	-33.6	76	-28	138	-24.8	200	-19.3	262	-6.5
16	-33.6	78	-27.8	140	-24.9	202	-19	264	-5.8
18	-33.5	80	-27.7	142	-24.9	204	-18.8	266	-5.2
20	-33.4	82	-27.6	144	-24.7	206	-18.4	268	-4.7
22	-33.2	84	-27.4	146	-24.5	208	-18		
24	-33.1	86	-27.2	148	-24.4	210	-17.7		
26	-32.8	88	-27.1	150	-24.3	212	-17.3		
28	-32.7	90	-26.9	152	-24	214	-16.7		
30	-32.4	92	-26.8	154	-24	216	-16.4		
32	-32	94	-26.7	156	-23.9	218	-16.2		
34	-31.8	96	-26.6	158	-23.7	220	-15.9		
36	-31.6	98	-26.4	160	-23.5	222	-15.5		
38	-31.3	100	-26.3	162	-23.3	224	-15.2		
40	-31	102	-26.2	164	-23	226	-14.8		
42	-30.9	104	-26.1	166	-22.7	228	-14.5		
44	-30.7	106	-25.9	168	-22.5	230	-14.3		
46	-30.5	108	-25.8	170	-22.3	232	-13.9		
48	-30.3	110	-25.7	172	-22.2	234	-13.6		
50	-30.1	112	-25.5	174	-22	236	-13.4		
52	-29.9	114	-25.4	176	-21.9	238	-13		
54	-29.8	116	-25.2	178	-21.8	240	-12.9		
56	-29.7	118	-25.1	180	-21.5	242	-12.7		
58	-29.5	120	-25.1	182	-21.4	244	-12.3		
60	-29.3	122	-25.1	184	-21.2	246	-11.8		

Table B-7, Freezing temperature profile for mixture of Decane and Dodecane

$0.8001C_{10} + 0.1999C_{12}$							
Freezing							
Time(min)	Sample Tp.^{o}C	Time(min)	Sample Tp.^{o}C	Time(min)	Sample Tp.^{o}C	Time(min)	Sample Tp.^{o}C
0	-20.6	62	-36.1	124	-38.5	186	-41.3
2	-21.2	64	-36.5	126	-38.5	188	-42
4	-22.1	66	-36.9	128	-38.6	190	-43.3
6	-22.8	68	-37.1	130	-38.5	192	-44.8
8	-23.5	70	-37.6	132	-38.7	194	-46.6
10	-24.3	72	-37.7	134	-38.7	196	-48.5
12	-24.7	74	-37.9	136	-38.8	198	-49.7
14	-25.4	76	-37.9	138	-38.8	200	-50.8
16	-26	78	-38	140	-38.9		
18	-26.7	80	-38	142	-38.9		
20	-27.2	82	-38	144	-38.9		
22	-27.7	84	-38	146	-39		
24	-28.1	86	-38	148	-39		
26	-28.6	88	-38.1	150	-39.1		
28	-29.2	90	-38.1	152	-39.2		
30	-29.6	92	-38.1	154	-39.2		
32	-30.1	94	-38.1	156	-39.3		
34	-30.4	96	-38.2	158	-39.2		
36	-31	98	-38.3	160	-39.3		
38	-31.4	100	-38.4	162	-39.2		
40	-31.9	102	-38.4	164	-39.2		
42	-32.2	104	-38.4	166	-39.3		
44	-32.7	106	-38.4	168	-39.3		
46	-33	108	-38.4	170	-39.2		
48	-33.5	110	-38.4	172	-39.2		
50	-33.8	112	-38.4	174	-39.3		
52	-34	114	-38.5	176	-39.5		
54	-34.4	116	-38.5	178	-39.7		
56	-34.7	118	-38.4	180	-39.9		
58	-35.4	120	-38.4	182	-40.2		
60	-35.7	122	-38.4	184	-40.6		

Table B-8, Melting temperature profile for mixture of Decane and Dodecane

$0.8001C_{10} + 0.1999C_{12}$					
Melting					
Time(min)	Sample Tp.^{o}C	Time(min)	Sample Tp.^{o}C	Time(min)	Sample Tp.^{o}C
0	-50.2	62	-34.8	124	-26
2	-48.7	64	-34.7	126	-25
4	-47.9	66	-34.7	128	-24.2
6	-46.5	68	-34.6	130	-23.6
8	-45.9	70	-34.6	132	-22.9
10	-45.2	72	-34.5	134	-22.2
12	-44.1	74	-34.4	136	-21.7
14	-43.2	76	-34.4	138	-21.2
16	-42.3	78	-34.3	140	-20.7
18	-41.7	80	-34.2		
20	-40.9	82	-34.1		
22	-40.4	84	-34		
24	-39.7	86	-33.9		
26	-39	88	-33.5		
28	-38.7	90	-33.3		
30	-38.4	92	-33.3		
32	-38	94	-33.1		
34	-37.4	96	-32.9		
36	-37.2	98	-33.1		
38	-36.7	100	-32.4		
40	-36.3	102	-31		
42	-36	104	-31.8		
44	-35.9	106	-31.8		
46	-35.7	108	-32		
48	-35.6	110	-31.1		
50	-35.5	112	-30		
52	-35.3	114	-29.6		
54	-35.2	116	-28.8		
56	-35.1	118	-28.4		
58	-35	120	-27.7		
60	-34.9	122	-27		

Table B-9, Freezing temperature profile for mixture of Decane and Dodecane

Freezing											
$0.8357C_{10} + 0.1646C_{12}$											
Time(min)	Sample Tp°C	Time(min)	Sample Tp°C	Time(min)	Sample Tp°C	Time(min)	Sample Tp°C	Time(min)	Sample Tp.°C	Time(min)	Sample Tp.°C
0	25.4	62	1.2	124	-9.9	186	-16	248	-20.9	310	-26.8
2	25.4	64	0.4	126	-10.1	188	-16.2	250	-21	312	-27.1
4	25.3	66	-0.5	128	-10.3	190	-16.5	252	-21.2	314	-27.4
6	24.8	68	-1	130	-10.5	192	-16.7	254	-21.4	316	-27.6
8	24.3	70	-1.7	132	-10.7	194	-16.8	256	-21.6	318	-27.8
10	23.8	72	-2.3	134	-10.9	196	-16.8	258	-21.8	320	-27.9
12	23.1	74	-2.7	136	-11.1	198	-16.9	260	-22	322	-28
14	22.4	76	-3.2	138	-11.3	200	-17.1	262	-22.2	324	-28.2
16	21.9	78	-3.8	140	-11.5	202	-17.1	264	-22.3	326	-28.4
18	20.8	80	-4.2	142	-11.7	204	-17.3	266	-22.5	328	-28.5
20	20.2	82	-4.6	144	-11.9	206	-17.4	268	-22.7	330	-28.7
22	19.5	84	-4.9	146	-12.1	208	-17.5	270	-23	332	-28.9
24	18.6	86	-5.3	148	-12.3	210	-17.6	272	-23.1	334	-29
26	17.8	88	-5.6	150	-12.4	212	-17.8	274	-23.3	336	-29.2
28	16.8	90	-5.9	152	-12.6	214	-18	276	-23.5	338	-29.4
30	16	92	-6.3	154	-12.8	216	-18.1	278	-23.7	340	-29.5
32	15.1	94	-6.5	156	-13	218	-18.2	280	-23.9	342	-29.8
34	14.2	96	-6.7	158	-13.2	220	-18.4	282	-24.1	344	-30
36	13.2	98	-7	160	-13.4	222	-18.6	284	-24.3	346	-30.3
38	12.3	100	-7.3	162	-13.6	224	-18.8	286	-24.5	348	-30.3
40	11.4	102	-7.5	164	-13.8	226	-18.9	288	-24.7	350	-30.5
42	10.5	104	-7.8	166	-14	228	-19	290	-24.9	352	-30.7
44	9.6	106	-8	168	-14.1	230	-19.3	292	-25.1	354	-30.8
46	8.6	108	-8.2	170	-14.3	232	-19.4	294	-25.3	356	-31.2
48	7.7	110	-8.4	172	-14.5	234	-19.6	296	-25.4	358	-31.2
50	6.7	112	-8.6	174	-14.7	236	-19.8	298	-25.6	360	-31.4
52	5.8	114	-8.9	176	-14.9	238	-20	300	-25.8	362	-31.7
54	4.8	116	-9.1	178	-15.1	240	-20.2	302	-26.1	364	-32
56	4	118	-9.2	180	-15.3	242	-20.4	304	-26.2	366	-32.3
58	3	120	-9.5	182	-15.5	244	-20.5	306	-26.4	368	-32.5
60	2.1	122	-9.7	184	-15.7	246	-20.7	308	-26.6	370	-32.7

Freezing			
$0.8357C_{10} + 0.1646C_{12}$			
Time(min)	Sample Tp°C	Time(min)	Sample Tp°C
372	-32.8	436	-37.5
374	-33.2	438	-37.6
376	-33.2	440	-37.6
378	-33.3	442	-37.6
380	-33.7	444	-37.6
382	-33.9	446	-37.8
384	-34	448	-37.8
386	-34.1	450	-38
388	-34.3	452	-38
390	-34.6	454	-38
392	-34.8	456	-38.1
394	-35		
396	-35.2		
398	-35.4		
400	-35.5		
402	-35.7		
404	-35.9		
406	-36.1		
408	-36.3		
410	-36.5		
412	-36.7		
414	-36.8		
416	-36.8		
418	-36.9		
420	-36.9		
422	-37		
424	-37		
426	-37.1		
428	-37.2		
430	-37.2		
432	-37.3		
434	-37.4		

Table B-10, Melting temperature profile for mixture of Decane and Dodecane

Melting											
$0.8357C_{10} + 0.1646C_{12}$											
Time(min)	Sample Tp°C	Time(min)	Sample Tp°C	Time(min)	Sample Tp°C	Time(min)	Sample Tp°C	Time(min)	Sample Tp.°C	Time(min)	Sample Tp.°C
0	-42.7	62	-38.9	124	-35.1	186	-32.8	248	-20.2	310	-12.7
2	-42.7	64	-38.7	126	-35	188	-32.8	250	-20	312	-12.6
4	-42.7	66	-38.5	128	-35	190	-32.8	252	-19.8	314	-12.5
6	-42.7	68	-38.4	130	-34.9	192	-32.7	254	-19.6	316	-12.4
8	-42.7	70	-38.2	132	-34.8	194	-32.6	256	-19.3	318	-12.3
10	-42.6	72	-38	134	-34.7	196	-32.5	258	-19.1	320	-12.1
12	-42.5	74	-37.9	136	-34.7	198	-32.3	260	-18.8	322	-11.9
14	-42.4	76	-37.8	138	-34.7	200	-32.1	262	-18.6	324	-11.7
16	-42.3	78	-37.6	140	-34.6	202	-31.8	264	-18.4	326	-11.6
18	-42.2	80	-37.4	142	-34.6	204	-31.8	266	-18.2	328	-11.4
20	-42.1	82	-37.3	144	-34.5	206	-31.1	268	-17.9	330	-11.3
22	-42	84	-37.1	146	-34.5	208	-30.6	270	-17.7	332	-11.1
24	-41.9	86	-37	148	-34.3	210	-30	272	-17.6	334	-10.9
26	-41.7	88	-36.9	150	-34.2	212	-29.5	274	-17.4	336	-10.7
28	-41.6	90	-36.8	152	-34.2	214	-28.3	276	-17.1	338	-10.6
30	-41.5	92	-36.7	154	-34.2	216	-27.4	278	-16.9	340	-10.4
32	-41.2	94	-36.5	156	-34.1	218	-26.9	280	-16.7	342	-10.2
34	-41	96	-36.4	158	-34	220	-26.1	282	-16.5	344	-10.1
36	-40.9	98	-36.3	160	-33.9	222	-25.2	284	-16.3	346	-10
38	-40.8	100	-36.1	162	-33.8	224	-24.7	286	-16	348	-9.6
40	-40.7	102	-36	164	-33.8	226	-24.2	288	-15.8	350	-9.5
42	-40.5	104	-36	166	-33.7	228	-23.7	290	-15.6	352	-8.9
44	-40.3	106	-35.9	168	-33.5	230	-23.2	292	-15.5	354	-8.6
46	-40.2	108	-35.7	170	-33.3	232	-22.9	294	-15.3	356	-8.4
48	-40	110	-35.6	172	-33.2	234	-22.4	296	-15	358	-8.2
50	-39.8	112	-35.6	174	-33	236	-22.1	298	-14.9	360	-8
52	-39.7	114	-35.4	176	-32.8	238	-21.7	300	-14.7	362	-7.9
54	-39.4	116	-35.3	178	-32.7	240	-21.4	302	-14.4	364	-7.7
56	-39.4	118	-35.3	180	-32.6	242	-21.1	304	-14.1	366	-7.5
58	-39.2	120	-35.1	182	-32.7	244	-20.8	306	-13.9	368	-7.3
60	-39	122	-35.1	184	-32.8	246	-20.5	308	-12.8	370	-7.3

Melting			
$0.8357C_{10} + 0.1646C_{12}$			
Time(min)	Sample Tp°C	Time(min)	Sample Tp°C
374	-6.8	430	15.4
376	-6.6	432	16.1
378	-6.4	434	17
380	-6.1	436	17.9
382	-5.4	438	18.6
384	-5	440	19.3
386	-4.2	442	20.4
388	-3.2	444	21
390	-2.3	446	21.6
392	-1.3	448	21.9
394	-0.4	450	22.1
396	0.5	452	22.3
398	0.9	454	22.4
400	1.8	456	22.6
402	2.8		
404	3.7		
406	4.9		
408	5.8		
410	6.5		
412	7.2		
414	8.1		
416	8.9		
418	9.7		
420	10.6		
422	11.4		
424	12.3		
426	13.5		

Table B-11, Freezing and melting temperature profile for mixture of Decane and Dodecane

$0.8988C_{10} + 0.1012C_{12}$									
Freezing						Melting			
Time(min)	Sample Tp.^{o}C	Time(min)	Sample Tp.^{o}C	Time(min)	Sample Tp.^{o}C	Time(min)	Sample Tp.^{o}C	Time(min)	Sample Tp.^{o}C
0	-19.9	62	-32.9	124	-33.7	0	-35.6	62	-32.3
2	-20.4	64	-33.3	126	-34	2	-35.2	64	-32.2
4	-20.9	66	-33.5	128	-34.1	4	-34.8	66	-32.1
6	-21.5	68	-33.7	130	-34.1	6	-34.5	68	-32
8	-21.9	70	-34	132	-34.2	8	-34.4	70	-32
10	-22.5	72	-34.4	134	-34.3	10	-34	72	-31.9
12	-23	74	-35	136	-34.4	12	-33.9	74	-31.8
14	-23.4	76	-35.4	138	-34.6	14	-33.7	76	-31.7
16	-23.9	78	-35.8	140	-34.6	16	-33.6	78	-31
18	-24.3	80	-36	142	-34.7	18	-33.5	80	-30.9
20	-24.7	82	-35.9	144	-34.8	20	-33.4	82	-30.4
22	-25.3	84	-35.5	146	-34.9	22	-33.3	84	-29.3
24	-25.6	86	-34.6	148	-35	24	-33.2	86	-27.9
26	-26	88	-34	150	-35	26	-33.1	88	-25.8
28	-26.5	90	-33.6	152	-35.2	28	-33.2	90	-24.2
30	-26.9	92	-33.3	154	-35.4	30	-33.1	92	-22.9
32	-27.2	94	-33.2	156	-35.7	32	-32.9	94	-21.6
34	-27.5	96	-33.1	158	-36	34	-32.9	96	-20.7
36	-27.9	98	-33.1	160	-36.3	36	-32.9	98	-19.8
38	-28.3	100	-33.1	162	-36.5	38	-32.8	100	-19
40	-28.7	102	-33.1	164	-36.8	40	-32.8	102	-18.4
42	-29.1	104	-33.1	166	-37.4	42	-32.7	104	-17.6
44	-29.4	106	-33.1	168	-38.3	44	-32.7	106	-16.8
46	-29.9	108	-33.2			46	-32.6	108	-16.3
48	-30.2	110	-33.3			48	-32.6	110	-15.8
50	-30.7	112	-33.4			50	-32.5	112	-15.2
52	-31	114	-33.4			52	-32.5		
54	-31.4	116	-33.4			54	-32.4		
56	-31.9	118	-33.5			56	-32.4		
58	-32.1	120	-33.6			58	-32.4		
60	-32.5	122	-33.6			60	-32.3		

Table B-12, Liquid Sample Composition at various Freezing Temperatures

	Decane	Dodecane	
Area of Initial Sample	7294.3656	1709.1874	
Moles @ Initial	3.57658E-09	7.02945E-10	4.27952E-09
Mole fraction @ Initial	**0.8357**	**0.1643**	
Area @ -10°C	6788.676	1559.9312	
Moles @ -10°C	3.32863E-09	6.4156E-10	3.97019E-09
Mole fraction @ -10oC	**0.8384**	**0.1616**	
Area @ -17°C	6927.5666	1593.3148	
Moles @ -17°C	3.39673E-09	6.5529E-10	4.05202E-09
Mole fracton @ -17°C	**0.8383**	**0.1617**	
Area @ -21°C	6875.5236	1591.4158	
Moles @ -21°C	3.37121E-09	6.54509E-10	4.02572E-09
Mole fraction @ -21°C	**0.8374**	**0.1626**	
Area @ -27°C	6946.2868	1581.4752	
Moles @ -27°C	3.40591E-09	6.5042E-10	4.05633E-09
Mole fraction @ -27°C	**0.8397**	**0.1603**	
Area @ -29°C	7010.292	1614.6932	
Moles @ -29°C	3.43729E-09	6.64082E-10	4.10137E-09
Mole fraction @ -29°C	**0.8381**	**0.1619**	

Table B-13, Liquid Sample Composition at various Melting Temperatures

	Decane	Dodecane	
Area of Initial Sample	7294.3656	1709.1874	
Moles @ Initial	3.5766E-09	7.0295E-10	4.2795E-09
Mole fraction @ Initial	**0.8357**	**0.1643**	
Area @ -33C	11374	2551	
Moles @ -33°C	5.5769E-09	1.0492E-09	6.6261E-09
Mole fraction @ -33°C	**0.8417**	**0.1583**	
Area @ -26°C	8187.3768	1826.0164	
Moles @ -26°C	4.0144E-09	7.5099E-10	4.7654E-09
Mole fraction @ -26°C	**0.8424**	**0.1576**	
Area @ -25°C	8768	1955	
Moles @ -25°C	4.2991E-09	8.0404E-10	5.1032E-09
Mole fraction @ -25°C	**0.8424**	**0.1576**	
Area @ -23°C	7587.2268	1713.3848	
Moles @ -23°C	3.7202E-09	7.0467E-10	4.4248E-09
Mole fraction @ -23°C	**0.8407**	**0.1593**	
Area @ -21°C	7452.422	1622.791	
Moles @ -21°C	3.6541E-09	6.6741E-10	4.3215E-09
Mole fraction @ -21°C	**0.8456**	**0.1544**	
Area @ -19°C	7513.7392	1624.61	
Moles @ -19°C	3.68414E-09	6.68161E-10	4.3523E-09
Mole fraction @ -19°C	**0.8465**	**0.1535**	
Area @ -17°C	11580.3512	2599.566	
Moles @ -17°C	5.6781E-09	1.0691E-09	6.7472E-09
Mole fraction @ -17°C	**0.8415**	**0.1585**	
Area @ -15°C	7172.5208	1629.7208	
Moles @ -15°C	3.5168E-09	6.7026E-10	4.1871E-09
Mole fraction @ -15°C	**0.8399**	**0.1601**	
Area @ -10°C	7421.1652	1638.9104	
Moles @ -10°C	3.6387E-09	6.7404E-10	4.3128E-09
Mole fraction @ -10°C	**0.8437**	**0.1563**	
Area @ -6°C	7433.4264	1672.2236	
Moles @ -6°C	3.6448E-09	6.8774E-10	4.3325E-09
Mole fraction @ -6°C	**0.8413**	**0.1587**	